JPRS-JST-90-045
22 OCTOBER 1990

FOREIGN
BROADCAST
INFORMATION
SERVICE

JPRS Report

Science & Technology

Japan

JPRS-JST-90-045
22 OCTOBER 1990

SCIENCE & TECHNOLOGY
JAPAN

CONTENTS

SCIENCE & TECHNOLOGY

SUPERCONDUCTIVITY

Comparing International Technological Capabilities

906C3849A Tokyo BOEI GIJUTSU in Japanese Dec 89 pp 37-48

[Article by Atsuhiko Banshou: "Critical Technology--Comparison of the Technological Levels of the United States and Other Countries"]

[Text] I have introduced the outline of the critical technology plan of the Department of Defense (DOD) of the United States in the June issue of DEFENSE TECHNOLOGY JOURNAL. In addition, I have introduced the outline and impact of 22 individual technologies on weapon systems, and the status of research and development carried out by DOD and organs other than the DOD in the July to November issues of DEFENSE TECHNOLOGY JOURNAL on the basis of attached data.

This report was first published on 15 March 1989, and the contents were introduced as mentioned above. Subsequently, a revised report was published on May 1989. The main revisions were the separation of the, "Overall Evaluation" chapter mentioned in the report from the "Status of Research and Development Carried Out by Organs Other Than the DOD" mentioned in the attached data, and the separation of "Relevant Research and Development Work in the United States" from "Comparisons with Other Countries." Particularly, details of the "Comparison with Other Countries" have been described in a series of this journal since the first edition. Also, the revision covers "Tables of Comparison with Capability of Foreign Countries with respect to each new technology. "Comparison with Other Countries" shows the present and future power of hostile countries and indicates opportunities for cooperation for mutual benefit of the United States and allied countries. I will describe here the contents of the "Overall Evaluation" and "Tables of Comparison with Capability of Foreign Countries" mentioned in the report.

Critical Technology Plan

E. Overall Evaluation

The main purpose of the science and technology plan of the DOD are still the development and application of new technologies, because present weapon systems increasingly rely on advanced technologies. As can be

seen from the advent of radar equipment and nuclear weapons in World War II and that of subsequent aerospace, electronic, and computer industries, and national defense demand has brought about unforeseen nonmilitary products and occasionally, quite new industries. According to the DOD's present plan, importance is attached to the direct support for research and development carried out by universities and industry, and such work carried out individually by the industry is arranged to promote the transfer of the work from the research stage to the operational.

Many countries make every effort to advance technologies. Table 1 shows results of overall evaluating 22 important technologies of our main allied countries, potential enemy countries, and some other countries. Each technology is evaluated in written form in the attached data. The United States continues to lead the world in these important technologies, but it is recognized that other countries have a capability equivalent to or greater than that of the United States, because they have progressed remarkably in important sections of some technologies. The attached data cover fields having a possibility of constructive cooperation.

Japan: Japan continues to lead the world and shares another lead with other countries in important sections of technologies for microelectronics, optics, superconductivity, and information systems. Japan is increasingly interested in the expansion of the foundation of military technologies and shows the intention of expanding it.

NATO: Our allies have powerful national plans and narrow gaps in some sections of each important technology. Accordingly, they have many opportunities for mutual cooperation. The progress for true unity of Europe in 1992 would raise NATO's capability together with a joint plan of information technologies, materials, and military systems, carried out positively by these other countries.

Table 1. Summary of Foreign Technological Capabilities

Critical Technologies	Warsaw Pact	NATO Allies	Japan	Others
1. Microelectronic Circuits and Their Fabrication	■	▨	▨	▨ Israel ▨ S. Korea
2. Preparation of GaAs and Other Compound Semiconductors	■	▨	▨	
3. Software Producibility	■	▨	▨	▨ Many Nations
4. Parallel Computer Architectures	■	▨	▨	
5. Machine Intelligence/Robotics	■	▨	▨	▨ Finland, Sweden
6. Simulation and Modeling	■	▨	▨	
7. Integrated Optics	■	▨	▨	▨ China, Israel, S. Korea
8. Fiber Optics	■	▨	▨	▨ Various Sources
9. Sensitive Radars	■	▨	▨	▨ Sweden
10. Passive Sensors	■	▨	▨	▨ Israel
11. Automatic Target Recognition	■	▨	▨	▨ Israel, Sweden
12. Phased Arrays	■	▨	▨	▨ Israel
13. Data Fusion	■	▨	▨	
14. Signature Control	■	▨	NA	
15. Computational Fluid Dynamics	■	▨	▨	▨ Sweden
16. Air-Breathing Propulsion	■	▨	▨	
17. High Power Microwaves	■	▨		
18. Pulsed Power	■	▨	▨	
19. Hypervelocity Projectiles	■	▨	▨	▨ Australia, Israel
20. High-Temperature/High-Strength/Low-Weight Composite Materials	■	▨	▨	
21. Superconductivity	■	▨	▨	
22. Biotechnology Materials and Processing	■	▨	▨	▨ Many Nations

Remarks:

Position of Warsaw Pact countries compared with the United States

■ Takes a considerable lead in a certain technical field

Capability of allied countries that can contribute to technologies

▨ Considerably Superior in a certain technical

■■■	Overall equivalent to the United States	▨▨▨	Can become a main contributor
■■	Lags behind in all the fields other than a certain field	▨▨	Can become a partial contributor
■	Lags behind in all the important fields	▨	Cannot be considered immediately to contribute

Table 1-1. Summary Comparison--Microelectronic Circuits and Their Fabrication

	Warsaw Pact	NATO Allies	Japan	Others
High-speed digital processing, either by use of submicron or unique geometries, or the use of GaAs or other high electron-mobility semiconductor materials	■	▨▨	▨▨▨	▨▨ Israel, Switzerland
Larger scale integration, to greater component densities or yield in large substrates	■	▨▨	▨▨▨	▨▨ Israel ▨ South Korea
Higher levels of functional integration, including MMIC and integration of analog/digital functions on a single substrate	■	▨▨	▨▨▨	▨▨ Israel
OVERALL EVALUATION	■	▨▨	▨▨▨	▨▨ Israel ▨ South Korea

Table 1-2. Summary Comparison--Preparation of Gallium Arsenide and Other Compound Semiconductors

	Warsaw Pact	NATO Allies	Japan	Others
Preparation of gallium arsenide and other compound semiconductor materials	■	▨▨	▨▨	
Development and growth of complex structures (e.g., strained superlattices) of compound semiconductor materials	■	▨	▨▨	
OVERALL EVALUATION	■	▨	▨▨	

Table 1-3. Summary Comparison--Software Producibility

	Warsaw Pact	NATO Allies	Japan	Others
Enhanced software development environments	■	▨	▨	
Operating systems and applications software to support real-time information management in large, distributed systems	■	▨	▨	
Algorithms, languages, and tools for advanced parallel architectures	■	▨	▨	▨ Note 1
OVERALL EVALUATION	■	▨	▨	▨

Note 1. Many countries have ongoing theoretical work in algorithms. Individual breakthroughs are possible from any of these efforts, but cannot be predicted or planned.

Table 1-4. Summary Comparison--Parallel Computer Architectures

	Warsaw Pact	NATO Allies	Japan	Others
Component development and production	■	▨▨	▨▨▨▨	
Computer architectural designs	■	▨▨	▨▨	
Hardware design and packaging, thermal management, power distribution, interconnection	■	▨▨	▨▨▨	
Specialized software engineering skills, especially those for supercomputing or advanced parallel architectures	■	▨▨▨▨	▨▨▨	
OVERALL EVALUATION	■	▨▨	▨▨	

Table 1-5. Summary Comparison--Machine Intelligence/Robotics

	Warsaw Pact	NATO Allies	Japan	Others
Development and use of smart sensors	■	▨▨▨	▨▨▨▨	
Specialized computing architectures, including neural networks	■	▨▨	▨▨	
Specialized software engineering skills, especially those for advanced parallel architectures	■	▨▨▨	▨▨▨	
OVERALL EVALUATION	■	▨▨▨	▨▨▨▨	▨▨ Finland ▨▨ Sweden (Note 1)
	Note 1. While not dominant in any key aspect of this technology, Finland and Sweden have reported research in speech and image processing algorithms that may be applicable to neural networks.			

Table 1-6. Summary Comparison--Simulation and Modeling

	Warsaw Pact	NATO Allies	Japan	Others
Advanced computing for real-time or faster performance				
Effective man/machine interface for design/training				
Specialized software engineering skills, especially those for large database management				
Empirically validated information bases in substantive areas of interest	(Note 1)			
OVERALL EVALUATION				

Note 1. Soviet knowledge of wargaming and experimental strengths (e.g., in aircraft gas turbines and hypervelocity wind tunnels) will not contribute significantly in this area until computational deficiencies are corrected.

Table 1-7. Summary Comparison--Integrated Optics

	Warsaw Pact	NATO Allies	Japan	Others
Materials and manufacturing techniques for integrated optics				China
Materials/manufacturing techniques for optical switching				
Optical interconnection techniques				Israel
Optical beam steering devices				
Two-dimensional spatial light modulators				
Computer-generated holographics				China
OVERALL EVALUATION				China, Israel

Table 1-8. Summary Comparison--Fiber Optics

	Warsaw Pact	NATO Allies	Japan	Others
Development of improved production methods for long ultra-low loss fibers	■	▨	▨▨▨	▨ Various Sources
Components and interconnections	■	▨▨	▨▨	
Characterization of non-linear properties of single mode fibers for sensors	■	▨▨	▨▨	
OVERALL EVALUATION	■	▨▨	▨▨▨	▨ Various Sources

Table 1-9. Summary Comparison--Sensitive Radars

	Warsaw Pact	NATO Allies	Japan	Others
Development and use of high resolution multi-spectral sensors	■	▨▨	▨▨	
High frequency/high resolution radar/laser radar	■	▨▨	▨▨	▨▨ Sweden (Note 1)
High throughput computational techniques	■	▨▨	▨▨	
OVERALL EVALUATION	■	▨▨	▨▨	▨▨ Sweden (Note 1)
	Note 1. While not predominant in any key aspect of this technology, Sweden has reported some interesting research in target characterization with high resolution laser radar.			

Table 1-10. Summary Comparison--Passive Sensors

	Warsaw Pact	NATO Allies	Japan	Others
Development of large focal plane arrays	■	▨	▨ Note 1	▨ Israel
Improved techniques for microwave and millimeter wave radiometry	■	▨	▨	
Application of superconductive sensors	■	▨	▨	
Development of techniques for multisensor data fusion	■	▨	▨	
OVERALL EVALUATION	■	▨	▨	▨ Israel
	Note 1. While not predominant in military IR detectors, Japanese capabilities could provide underlying technologies in compound semiconductors and fabrication of large focal plane arrays.			

Table 1-11. Summary Comparison--Automatic Target Recognition

	Warsaw Pact	NATO Allies	Japan	Others
Development of improved smart sensors	■	▨	▨	
High speed signal and data conversion	■	▨	▨	
Empirically validated engineering databases on targets and clutter clutter	■	▨	▨	
OVERALL EVALUATION	■	▨	▨	▨ Israel ▨ Sweden Note 1)
	Note 1. Sensitive nature of ATR technology may limit cooperative opportunities. However, Japanese technologies described in Sections 1 and 2 could contribute to critical component developments.			

Table 1-12. Summary Comparison--Phased Arrays

	Warsaw Pact	NATO Allies	Japan	Others
Development of conformal arrays	■	▨	▨	
Development of low-frequency active sonar	■	▨	▨	
Techniques for exploiting advanced parallel architectures	■	▨	▨	
OVERALL EVALUATION	■	▨ (Note 1)	▨ (Note 2)	▨ Israel

Note 1. While not predominant in any key aspect of this technology, the UK and France have specific capabilities of interest.

Note 2. In comparison to the United States, Japan has limited experience in fielding operational phased array radars. Their experience in gallium arsenide could, however, make a significant contribution to US development of active phased arrays.

Table 1-13. Summary Comparison--Data Fusion

	Warsaw Pact	NATO Allies	Japan	Others
Modeling of complex systems	■	▨	▨	
Algorithms for real-time analysis and correlation	■	▨	▨	
Development of gigabit/second or faster data links	■	▨	▨	
OVERALL EVALUATION	■	▨	▨	

Note. Despite obvious capabilities in underlying component technologies, and especially in fiber optic data links, Japan has limited experienced in practical applications of data fusion to tactical military problems.

Table 1-15. Summary Comparison--Computational Fluid Dynamics

	Warsaw Pact	NATO Allies	Japan	Others
Advanced computing capabilities	■	▨	▨▨	
Development of algorithms for advanced processors	■	▨	▨	▨ Sweden
Application-specific models and empirically valibated databases	■	▨	▨	
Specialized database management software for large engineering databases	■	▨	▨	
OVERALL EVALUATION	■	▨	▨	▨ Sweden

Table 1-16. Summary Comparison--Air Breathing Propulsion

	Warsaw Pact	NATO Allies	Japan	Others
Development and application of advanced high-temperature materials	■	▨	▨	
Modeling and simulation and empirically validated databases therefor	■	▨	▨	
OVERALL EVALUATION	■	▨	▨	

Table 1-17. Summary Comparison--High Power Microwaves

	Warsaw Pact	NATO Allies	Japan	Others
Development of high power microwave components				
Power handling and control for beam pointing and tracking				
OVERALL EVALUATION				

Table 1-18. Summary Comparison--Pulsed Power

	Warsaw Pact	NATO Allies	Japan	Others
Development of high energy-density storage devices and systems				
High-speed switching and power control devices				
OVERALL EVALUATION	(Note 1)		(Note 2)	
	Note 1. The Soviets have developed a number of alternative technological approaches. They are overall on a par with the US. Note 2. Strong in primary power sources that may prove adaptable to pulse power applications.			

Table 1-19. Summary Comparison--Hypervelocity Projectiles

	Warsaw Pact	NATO Allies	Japan	Others
Development of launchers and associated power systems				
Projectiles and projectile dynamics				Australia, Israel
Impact engineering and penetrative characteristics	(Note 1)			
OVERALL EVALUATION				
	Note 1. Hypervelocity > 20 km/sec			

Table 1-20. Summary Comparison--High-Temperature/High-Strength Light-Weight Composite Materials

	Warsaw Pact	NATO Allies	Japan	Others
Ability to produce material to specified performance levels				
Development of application-specific know-how				
OVERALL EVALUATION				

Table 1-21. Summary Comparison--Superconductivity

	Warsaw Pact	NATO Allies	Japan	Others
Development and fabrication of HTS materials				
Effective application of LTS materials	(Note 1)			
OVERALL EVALUATION	(Note 2)			

Note 1. The Soviets have developed a number of alternative techniques to circumvent specific problems. The Soviets lead the US in LTS research, development, and potential application.

Note 2. Strong in conversion and conditioning of power sources that may prove adaptable to pulse power applications.

Table 1-22. Summary Comparison--Biotechnology Materials and Processing

	Warsaw Pact	NATO Allies	Japan	Others
Development and fabrication of real-time detection and identification of biological/chemical agents				
Bioprocessing for decontamination and remediation				
Development of biomaterials for specific applications				
OVERALL EVALUATION				Numerous Countries (Note 1)

Note 1. Because of its pervasive importance in fundamental health and agricultural industries and the open dissemination of technology, research in biotechnology is virtually worldwide.

High-Resolution TFT-LCD for Cockpit Use

906C3849B Tokyo BOEI GIJUTSU in Japanese Dec 89 pp 49-55

[Article by Junji Kondo and Makoto Shibusawa, both presently engaged in development and design of active matrix LCD in Electron Device Engineering Laboratory, and Nobuo Hayashi and Yoshimasa Adachi, both presently engaged in development of technologies for actually installing LCD in Electron Device Engineering Laboratory: "High-Resolution TFT-LCD Module for Aircraft Cockpit Use"]

[Text] There is a high demand for graphic displays to replace conventional mechanical indicators used for multi-purpose indications in aircraft cockpits.

Toshiba has developed a 3.2-inch-diagonal TFT (thin film transistor) -LCD module with high resolution for use as an indicator in aircraft cockpits. The new module features horizontal and vertical pixel pitches of only 120 μm to provide the required level of display quality, and is also highly compact thanks to the use of advanced TAB (tape automated bonding) assembly techniques.

This paper describes some of the features of the TFT-LCD module, focusing on the design of the high-resolution TFT-LCD and the compactness of the module.

1. Preface

A very large number of mechanical indicators are installed in aircraft cockpits. In recent years, however, graphic displays have been used on a trial basis, primarily because multipurpose graphic displays can sharply reduce the number of necessary indicators. Furthermore, a high-resolution graphic display will become essential in the cockpit, because a traffic alert and collision avoidance system (TCAS) will soon be required in all civil aircraft operating in the United States.

The TCAS requires a multicolor indication display. The compact size and full color range of the LCD make it a promising candidate for such a display.

We have developed a high-resolution compact TFT-LCD module for cockpit displays. The screen is 3.2 inches on the diagonal, and the display size corresponds to a compact indication meter called "3-inch air transport indicator" (3ATI).

The TFT-LCD is a liquid display in which a thin film transistor as an active element for a switch is set in each pixel; this is an "active matrix type display." Compared with simple matrix liquid displays, the TFT-LCD has the advantage of indications with high resolution at high contrast. In recent years, TFT-LCD's with a diagonal of 3 to 5 inches or so have been successfully commercialized for full-color compact TV's, and we have already produced TFT-LCD's for compact TV's with diagonals of 2.7 and 4 inches. On the other hand, our new TFT-LCD module is called "display for aircraft cockpit use."

This module was developed with the aim of finding new uses for TFT-LCD's. We will now describe features of the module, especially the design of the high-resolution TFT-LCD.

2. Basic Operation of TFT-LCD

Figure 1 shows an equivalent circuit of a pixel section of a TFT-LCD. Data on a signal conductor are accumulated in an auxiliary capacity and a liquid crystal, forming the capacity of a pixel section, because the TFT is on as long as gate pulses are applied to the TFT and the signal conductor and pixel electrode are conductive. (This is called "writing.")

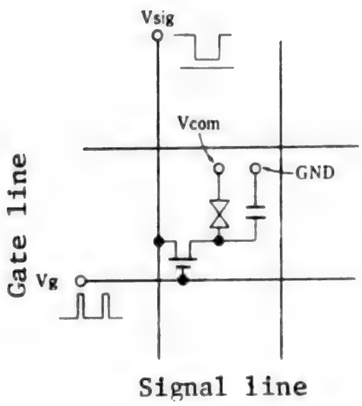

Figure 1. Equivalent Circuit of TFT-LCD Pixel Section

A pixel consists of TFT, liquid crystal capacity, and auxiliary capacity.

The liquid crystal is subjected to voltage equivalent to a potential difference between data signals and potential (Vcom) common to facing substrates. Next, ideally accumulated voltage is retained until gate pulses are applied to the pixel. Basically, the TFT-LCD is operated by repeating the writing and retaining processes. It is possible to express the brightness by properly changing the value of data signals, because as shown in Figure 2, the transmittance of liquid crystals depends on voltage applied to these liquid crystals. Also, the polarity of voltage is impressed on liquid crystals every field. In order to prevent these liquid crystals from being deteriorated, it is necessary to give data signals concerning the reverse rotation of this polarity to the liquid crystals.

3. Outline of Module

Table 1 outlines module specifications. Features of this module are as follows:

(1) High Resolution

Basically, the meter indication is graphic, and high resolution is required in indication patterns. The module contains 230,400 pixels (480 x 480), each pixel is very small (120 x 120 μm), and the resolution is high. Also, the aspect ratio of the screen is 1:1 from the standpoint of characters of the module, because the module was designed to be an alternate for a meter which was originally round.

(2) Quadratic Pixel Array

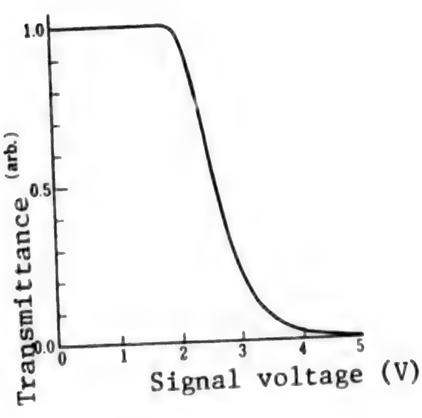

Figure 2. Transmittance of TFT-LCD and Signal Voltage Characteristics

Brightness can be expressed by changing signal voltages.

Table 1. Specifications of TFT-LCD Module

Indication area	57.6 x 57.6 mm
Number of pixels	480 x 480
Pixel pitch	120 x 120 μm
Pixel array	Quadratic array
Indication mode	Transmission type, normally white
Driving method	Noninterlace line sequence driving
Outside dimension of module	77.8 x 77.8 x 17.5 mm

The delta pixel array is used for TV indications, but the quadratic pixel array is used in this module (Figure 3). This is because the module was designed not to distort the character and graphic displays in consideration of the meter display. This matter is considered in the color array of color display modules.

(3) Compact Module

Skillful design of the module yielded the maximum indication area in the limited space.

(4) High Light Resistance

Light resistance is enhanced by using a color filter with a special structure, and exterior light resistance is also enhanced by creating a surface antireflection film on the surface.

4. Design of Each Section of Module

4.1. Design of TFT Array

Figure 4 shows a cross section of a TFT with "reserve stagger structure." The TFT is structured so that scanning gate lines are arrayed on the lower side and signal lines for supplying data are arrayed on the upper side. At present, this structure is used widely in TFT-LCD's. Also, a small number of photoengraving processes (PEP's) are required in manufacturing TFT arrays, because a back channel cut system is used to form a channel section and no protecting layer is provided on the amorphous silicon which is so-called etching stopper. Now, the W/L is 28/10. The TFT array section is designed in accordance with the following principles.

(a) Increase in numerical aperture. As mentioned above, the pixels are very small, but the pattern size, etc., are lower-limited, because of requirements for processes. Accordingly, among TFT-LCD's with the same indication area, the smaller the pixels, the lower the rate (numerical aperture) accounted by the effective region. This lowers the luminance

R	G	R	G	R	G
G	B	G	B	G	B
R	G	R	G	R	G
G	B	G	B	G	B
R	G	R	G	R	G
G	B	G	B	G	B

(a) RGBG type

R	G	R	G	R	G
W	B	W	B	W	B
R	G	R	G	R	G
W	B	W	B	W	B
R	G	R	G	R	G
W	B	W	B	W	B

(b) RGBW type

Figure 3. Pixel and Color Array

The quadratic array is used in this module, because character and graphic displays predominate.

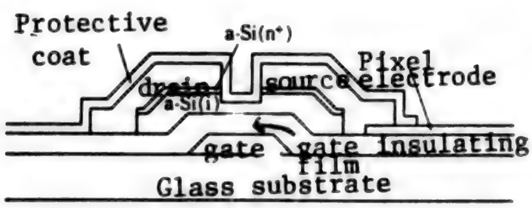

Figure 4. Structure of TFT Array

Reverse Stagger structure: W (channel width)/L (channel length) = 2.8

of screens. Therefore, the TFT array was designed to maximize the numerical aperture. As a result, this device has high resolution, as well as a high numerical aperture of about 40 percent.

(b) Rationalization of Auxiliary Capacity. The auxiliary capacity (Cs) is provided in parallel with liquid crystals. This capacity not only enhances the retaining capability, but also effectively relaxes the change of pixel potential by the parasitic capacity during TFT switching and decreases flicker. That is, the capacity is useful for raising the indication performance.[2] On the other hand, the increase in auxiliary capacity will cause some problems such as decrease in numerical aperture, increase in load during writing, etc. Considering the

advantages and disadvantages of the additional/auxiliary capacity, this module was designed with a large Cs while lowering the numerical aperture as little as possible.

4.2. Design of Color Filter

4.2.1. Structure of Black Matrix

The periphery of each pixel is surrounded by black matrixes on the substrate (color filter) facing the TFT array substrate. Such black matrixes are often formed with metallic films. On the other hand, as shown in Figure 5, the black matrix of the color filter used in this module has a unique structure in which a chromium layer is sandwiched between chromium oxide layers.

The amorphous silicon forming the TFT is light sensitive, but an increase in light leak current will decrease the indication contract at the lower portion of the screen and increase cross talk. Also, cockpits may be exposed to intense, direct sunlight at about 10,000 meters, and when this sunlight is reflected by black matrixes, it will obstruct viewing of the indication. In the black matrixes of this module, the chromium layer blocks light emitted from the back light, and the chromium oxide layer minimizes the influence of reflected external light and of back light reflected on the surface of the chromium layer. The back light is prevented from lowering the contrast ratio, and the high contrast ration is maintained even in intense light, because the light leak current of the TFT is reduced during the retaining operation.

4.2.2. Color Array

As shown in Figure 3, two kinds of color arrays were prepared for this module. In the red, green, blue, and gray (RGBG) pixel array shown in Figure 3(a), the number of G pixels is twice that of the R and B pixels. Accordingly, this array needs a back light in which the G peak of radiation spectra is lowered, but it is possible to indicate halftones. On the other hand, when one of the G's in the RGBG pixel array is changed to a gray filter, a red, green, blue, and white (RGBW) pixel array shown in Figure 3(b) will be obtained. An advantage of this array is that a typical three-wavelength tube can be used as a back light, and the transmittance of white cells can be enhanced more than in the RGBG pixel array, depending on the transmittance of the gray filter. However, the array is unsuitable for full-color indication.

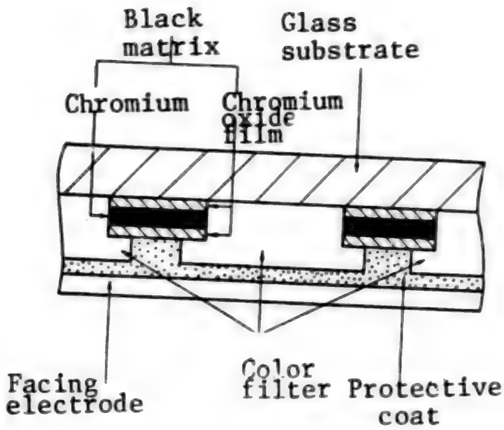

Figure 5. Structure of Black Matrix of Color Filter

Light resistance is increased with a three-layer structure consisting of chromium oxide, chromium, and chromium oxide.

The gray filter is formed by mixing the same kinds of pigments as those used in other R, G, and B pixel sections and is designed so that when a three-wavelength tube is used as a back light, the chromaticity of only white pixels will accord with that of a white color to which R, G, and B pixels are added.

4.3. Design of Liquid Crystal Cells

Liquid crystal layers in this module are 5.5 μm thick, because this thickness affects the transmittance of cells, angle of field, and yield. The liquid crystal used in the module is twisted nematic (TN), the orientation is of the rubbing type, and polyimide is used in oriented films. Polarizing plates were arranged so that they are of normally white modes, because although the meter indication is based on black, it is difficult to sufficiently indicate black with normally black modes. Also, the liquid crystal cell consists of TFT array substrate and facing substrate (color filter). Glass plates are attached to the polarizing plates on both sides of the liquid crystal cell to preventing deterioration of the polarizing plates, which are sensitive to humidity. In addition, films preventing surface reflection are on the indication face to improve readability in intense light.

4.4. Design of Module

The outside dimension of the liquid crystal cell is 72.0 x 72.0 mm, while that of the module is 77.8 x 77.8 mm. The module is a very compact 17.5

mm high and weighs about 100 grams. The following features made this compact design possible:

(1) high-density connection technology,

(2) installation of vertical bending TAB, and

(3) bending of the metallic base substrate

The aluminum base substrate was used as an external frame of the module without any change by wiring the aluminum base substrate, by bending this substrate, and by reinforcing a part of the substrate with stainless steel. This is the most important feature in the miniaturization of the module. In addition, a connection technology at a pad pitch of 200 μm was established by using an anisotropic conducting film (ACF). Four driver IC's for scanning lines and four for data are mounted on this substrate by installing the vertical bending TAB. Parts other than these IC's, including the control IC, are on another substrate, and both substrates are connected by a flexible cable. Figure 6 [omitted] shows a module.

4.5. Driving Method

The scanning method is in sequence from non-interlace lines. The frame frequency was determined to be 60 Hz. However, the writing time, i.e., the time in which the TFT is off, is about 34 μs, because there are 480 scanning lines; this time is much shorter than that for TV (about 64 μs). Otherwise, the driving method is almost the same as that for TV.

5. Operating Characteristics

Figure 7 shows the dependence of the contrast ratio on "viewing angle". The peak of the contrast ratio is in a point deviated slightly from the normal direction for the panel, and the value of this peak is 100:1 or more in weak surrounding light. The viewing angle that satisfy a contrast ratio of 10:1 or more range about 90 degrees horizontally and 60 degrees vertically.

Also, to install the module in an aircraft cockpit, observation of the indication must not be obstructed even when direct sunlight strikes the face. This module is designed so that the contrast ratio is 3:1 or more when the intensity of external light is 100,000 Ix without any cell surface antireflection film. The response time is 30 ms or less at normal temperatures. Also, the module is designed so that response time is not dependent on the viewing angle, thus eliminating distortion of the indication.

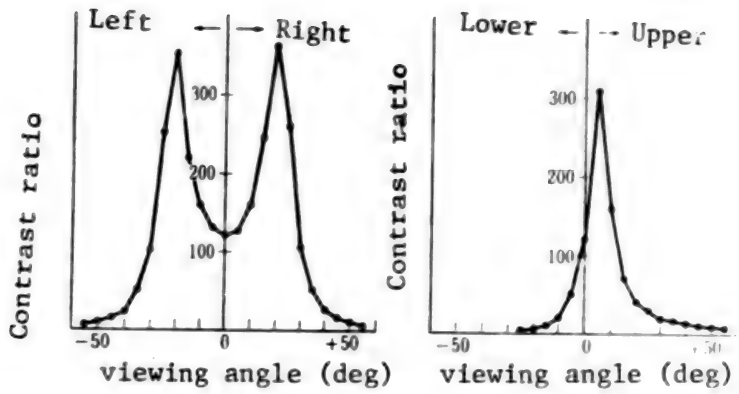

Figure 7. Dependence of Contrast Ration on Viewing Angle

The viewing angles that satisfy a contrast ration of 10:1 or more are horizontally about 90 degrees and vertically about 60 degrees.

6. Summary

We have developed a new high-resolution TFT-LCD compact display module for aircraft cockpit gauges (3ATI). It is expected that this module will be applied to aircraft TCAS, and in the future, the module may acquire the many indicating functions necessary for cockpits.

References

1. M. Shibusawa, et al., "A 212-Line/in. Full-Color TFT-LCD for Cockpit Use," SID '89 DIGEST, p 230 (1989).

2. T. Yanagisawa, et al., "Compensation of the Display Electrode Voltage Distortion," PROC. OF THE SID, 29(1), p 99 (1988).

High-Temperature Superconductors

906C3849C Tokyo BOEI GIJUTSU in Japanese Mar 90 pp 56-57

[Article by Yoshiroh Murayama of NEC Corporation: "Oxides High Temperature Superconducting Materials"]

[Text] It has been two years or more since the discovery of high-temperature superconductivity, but research on superconducting materials continues unabated. For example, new substances based on Bi (Tc= 107 degrees Kelvin) and based on Tl (Tc = 120 degrees Kelvin) were discovered in 1988. These substances show higher critical temperatures. NEC Corporation has undertaken basic research such as synthesis, analysis of structure, and evaluation of physical properties of these new substances and has attempted to develop thin film technologies that can apply the new substances to electronic fields.

The photograph [omitted] shows a high-resolution picture of $Ti_2Ba_2CuO_6$ taken with an electron microscope, and the black point is a metallic atom. It was discovered from this substance that the critical temperature was changed sharply from 0 to 80 degrees Kelvin by slight lattice defects. Electron microscopes are used to observe such substances, because it is difficult to clarify such crystal lattice defects by X-ray analysis. After measuring an energy gap that is a basically physical property of superconducting materials based on Y, Bi, and Tl, a value of $2\Delta/K_BT_C \fallingdotseq 6$ was obtained from all the superconducting materials (Figure 1). This value is different from that (3.5) obtained from the conventional BCS theory and suggests the possibility of new mechanisms. $TlBa_2YCu_2O_7$ is obtained by changing a part of a superconducting material based on Tl and is an antiferromagnetic substance. This fact was confirmed for the first time in the world in collaboration with Brookhaven National Laboratory in the United States. The fact strongly supports superconducting mechanisms based on magnetically mutual actions, which have recently come into the limelight.

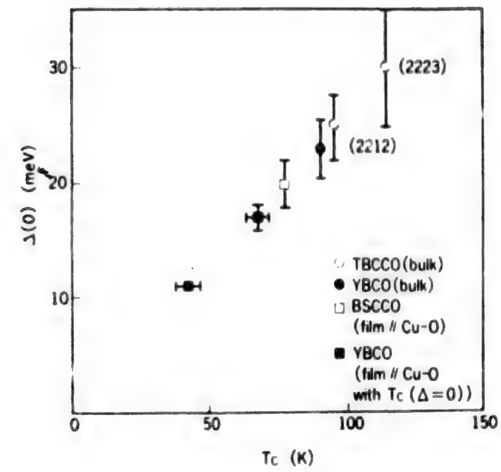

Figure 1

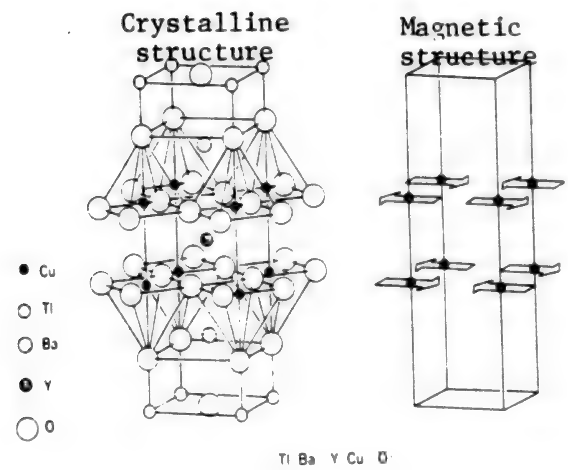

Figure 2

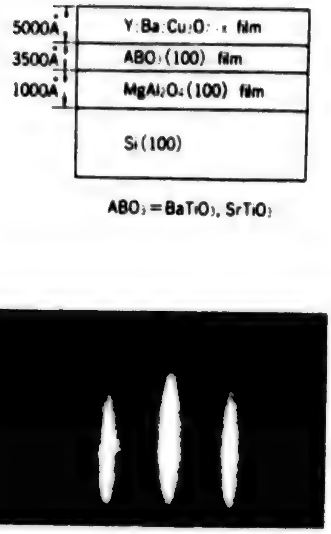

Figure 3

Epitaxial growth on silicon wafers has been one of the most important subjects in thin film technology, and NEC Corporation has succeeded in developing a new structure having a double layer consisting of $MgAl_2O_4$ spinel and $BaTiO_3$ as an intermediate layer. Figures 3 shows a thin film based on an epitaxial Y on a silicon wafer--its structure (upper portion) and its RHEED image (lower portion). As a result of research in collaboration with Bellcore Co., Ltd. in the United States, we have obtained a critical current density of 60,000 amperes per square centimeter (liquid nitrogen temperatures), the highest value up to now from thin films based on Y as films on silicon.

Adaptive MTI

906C3849D Tokyo BOEI GIJUTSU in Japanese Mar 90 pp 65-66

[Article by Mitsubishi Electric Corporation: "Adaptive Moving Target Indicator"]

[Text] Radar equipment simultaneously receives unnecessary echoes (clutter) reflected from background terrain, rain, clouds, etc., as well as echoes reflected from a target. Accordingly, it is necessary to use a filter to restrain such unnecessary echoes and extract only the echoes reflected from the target.

The moving target indicator (MTI) is a filter for restraining stationary clutter--echoes reflected from stationary background like the terrain--which has already been developed and put to practical use. In addition, some filters for restraining moving clutter--echoes reflected from moving background such as rain, clouds, etc.--are in use, but they are operated manually and frequently depend on the skill of the operators. Now, Mitsubishi Electric Corporation (MEC) has developed an adaptive moving target indicator (AMTI), which is an adaptive filter for automatically restraining such moving clutter.

If such AMTI's are connected continuously at multiple stages, they will be able to restrain simultaneously a number of moving clutter whose Doppler frequency is unknown. Also, the AMTI is designed not to restrain any echoes reflected from a target by using the difference between the spatial energy distribution of echoes reflected from the target and that of moving clutter.

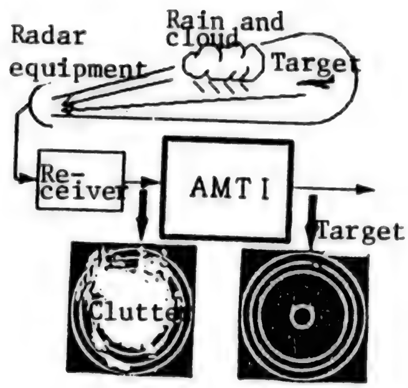

Figure 1. Performance of AMTI

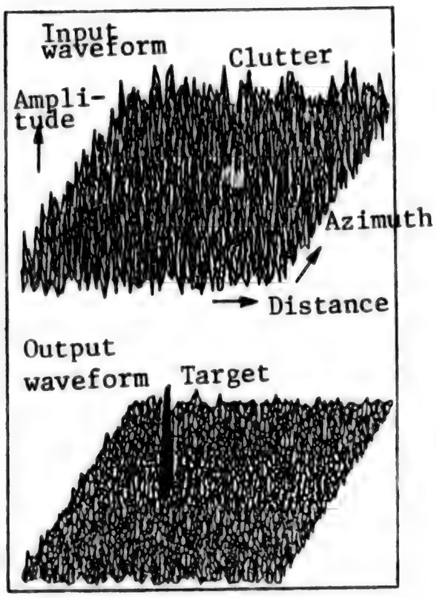

Figure 2. Example of Results of Experiment

MEC has conducted an experiment by using actual radar signals and has confirmed a moving clutter restraining performance of about 20 decibels.

(Extracted from MEC TECHNICAL JOURNAL, Vol 64, No 1, 1990)

Second Intelligent FA Symposium

Walking Robot Performance

906C0020 Tokyo INTELLIGENT FA SYMPOSIUM in Japanese 19 Jul 89 pp 23-26

[Article by Tatsuya Nakamura, Mechanical Engineering Laboratory, Agency of Industrial Science and Technology, MITI: "B2 Proposal of Indexes for Evaluating Performance of Walking Robot"]

[Text] Performance evaluation of walking robots from a viewpoint of a transportation means is important for walking robots to be practically accepted. So the performance measures used for automobiles and aircraft are reviewed and compared with those used in walking robot research. Based on these results, the following performance measures for walking robots are proposed: energy efficiency, stability, terrain adaptability, mobility, maximum speed, etc. Also, evaluation of several measures is conducted using a 3D dynamic simulator being developed in our laboratory.

1. Introduction

To establish the walking robot as a new means of transportation, it is necessary to be able to compare not only the performance of one walking robot with another, but also the performance of walking robots with other means of transportation. Generally, walking robots are said to excel in their ability to travel uneven ground but are inferior to other means of transportation in many respects including energy efficiency and speed. However, their utility cannot be determined and the definite target for developing them cannot be met unless a trade-off in these abilities is made quantitatively.

The themes of the MITI project "Robot for Critical Work" (1983-1990) include the development of a maintenance robot for nuclear power plants, etc., and the walking robot has been adopted as a means of transportation there. The study is being conducted as a "robot evaluating technology" and to simulate and evaluate the walking robot under various environments and help develop it. Quantification of robot evaluating indexes is one of the tasks involved.

In this announcement, I propose walking robot evaluating indexes that not only take indexes proposed in past walking robot studies into consideration but also are consistent with the performance evaluating indexes for other means of

transportation. But here, the object is performance commonly known as kinetic performance and other specification data, such as payload, are excluded.

2. Survey on Evaluating Indexes

We studied the kinetic performance of mobile machines from the viewpoints of energy electric field, stability, environment adaptability, and manuverability. Below are the results of the study done by referring to the Automobile Engineering Handbook and the Aerospace Engineering Handbook for automobiles and aircraft and to research papers for walking robots. Table 1 shows main evaluating indexes.

Table 1. Comparison of Main Kinetic Performance Evaluating Indexes

Item	Walking robot	Automobile	Aircraft
Energy efficiency	Locomotion power	Fuel consumption rate	Range performance
Stability	Margin of stability Dynamic stability	Maximum stability inclination	Static stability Stalling speed Dynamic stability
Environment adaptability	Terrain adaptability	Hill climbing capacity	Possible flying range
Maneuver-ability	Maximum locomotive speed	Automobile performance diagram Braking distance Minimum turning radius Accelerating capacity	Maximum flying speed Climb performance Landing performance Take-off performance

(1) Energy efficiency[1]: All are identical in substance, but are expressed differently. So, energy efficiency can be compared between different means of transportation. Comparison of energy efficiency between different means of transportation was done by von Karman[2] but, for walking, he referred to living things. Lately, some have begun comprehensive walking robot efficiency evaluation involving the actuator.

(2) Stability: As a common evaluating index, there is static stability, and in all cases the center of gravity is involved. As for the concept of dynamic stability, there is something in common between walking and aircraft. For example, the characteristic of θ displacement from the state of equilibrium, is expressed by a secondary vibration system

$$\theta + 2\zeta\omega\theta + \omega^2\theta = 0$$

and stability is discussed by ζ.

(3) Adaptability to environments: Pertinent indexes are defined for both automobiles and aircraft. As for the walking robot, there has been a study with the notion that it properly excels in terrain adaptability but its evaluating index is still not quantitative.

(4) Maneuverability: This is performance related to speed and acceleration. Examples: fast locomotion, quick correspondence and small turning radius. However, no index related to acceleration has yet been adopted for the walking robot.

3. Proposal of Evaluating Indexes

I propose performance evaluating indexes for the walking robot in accordance with the above survey. An independent index is used for the maximum locomotive speed and maneuverability is limited to performance related to acceleration.

(1) Locomotion efficiency:

- $\textit{Locomotion power} = \dfrac{\textit{Consumed energy}}{\textit{Weight x travel}}$

(2) Stability:

- $\textit{Allowance of static stability} = \dfrac{\textit{Allowance of the center of gravity displacement}}{\textit{Standard length}}$

- Allowance of dynamic stability = Stability allowance of restoration time (using conception of control)

(3) Terrain stability:

- Maximum inclination permitting hill climbing

- Maximum degree of uneven ground permitting locomotion

(4) Maneuverability:

- Time required for turning

- Acceleration performance

(5) Maximum locomotion speed

(6) Others:

- Controllability, etc.

Item (6) Others, includes indexes, too early to be defined now, and which should be defined with a view to the future progress of walking robot technology.

4. Example of Evaluation

The target of this study is to prepare an evaluation simulator prototype. We have already prepared a three-dimensional dynamics simulation basic program[5] but, since there is no complete program available to simulate how the legs hit and slide on the floor, only the simulation of static walking is possible now.

In this announcement, therefore, stability and locomotive power were evaluated for straight crawl walking with a duty factor of 0.8. Figure 1 shows the mechanism of the four-foot walking robot that was simulated. Also, the following specifications were set:

<Trunk> Weight: 20 kg; size: 1 m x 0.4 m

<Legs> Weight: 0.9 kg each; length: 0.9 m

In computing energy, the efficiency of the actuator and the transfer system was ignored and approximation was made by the sum of $\int | \tau \omega | dt$ for joint torque τ and angular velocity ω. Stability/instability was determined by whether the ground reaction of the grounding leg was positive or negative. Furthermore, the ground reaction distribution of the equilibrium force field[6] was used to determine the distribution of joint torques.

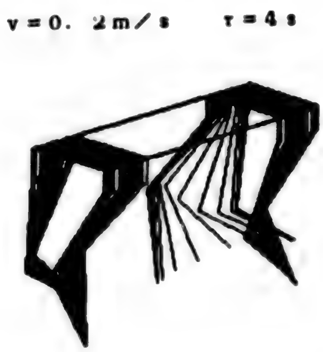

Figure 1. Example of Simulation of Walking Robot

Table 2 shows the results of simulation of some locomotion speeds and cycles and Figure 2 shows the results of entry of per-hour consumed energy obtained into a von Karman drawing. From this, one can see that the results are appropriate.

Table 2. Example of Evaluation of Locomotive Power and Stability

Locomotion speed	0.1 m/s				0.2 m/s		
Cycle (s)	2	3	4	6	2	3	4
Length of step (m)	0.16	0.24	0.32	0.48	0.32	0.48	0.64
Stability	Un-stable	Stable	Stable	Stable	Un-stable	Stable	Stable
Locomotion power	-	0.225	0.217	0.208	-	0.147	0.146

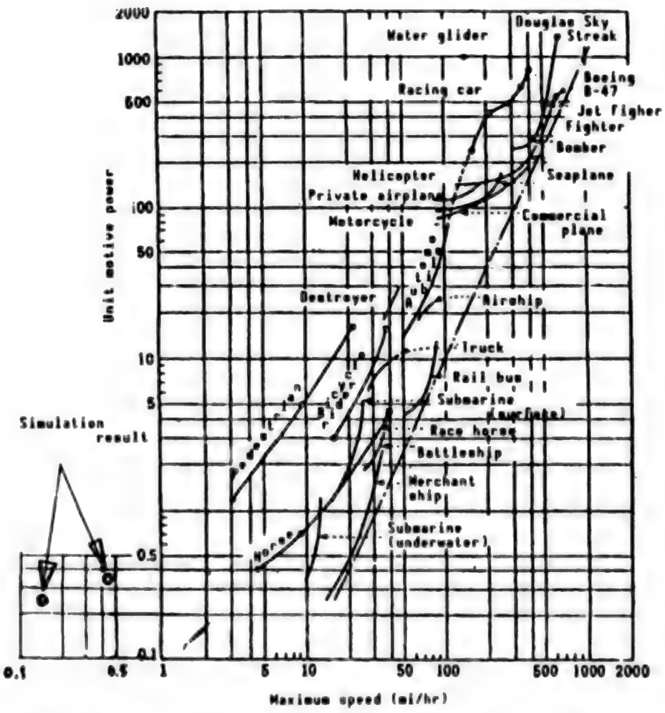

Figure 2. Results of Simulation and Comparison With Other Means of Transportation[2]

5. Summary

We experimented with quantitative walking robot performance evaluation indexes mainly on the basis of literature search, paying special attention to matching with other means of transportation. Examples of evaluation shown are still only partial. We will hereafter seek to expand our simulation programs so that the indexes proposed in this announcement can be evaluated.

References

1. Hirose and Umetani, "Basic Study Concerning Energy Efficiency of Walking Machine," (KEI-JI-RON), Vol 15 No 7, 1979, pp 928-933.

2. Von Karman, "Hiko no Riron (Theory of Flight), Iwanami, 1956, p 158.

3. Kimura, Shimoyana, and Miura, "Dynamic Analysis of Four-Foot Walking Robot," JOURNAL OF ROBOTIC SOCIETY OF JAPAN, Vol 6 No 5, 1988, pp 367-379.

4. Messuri, D.A. and Klein, C.A., "Automatic Body Regulation for Maintaining Stability of a Legged Vehicle During Rough-Terrain Locomotion," IEEE J. ROBOTICS AND AUTOMATION, Vol RA-1 No 3, 1988, pp 333-334.

5. Nakamura, Adachi, Koyauchi, and Nagata, "Method of Three-Dimensional Simulation of Walking Robot," 31st Automatic Control Federation Lecture Meeting, 1988, pp 333-334.

6. Kumar, V.R. and Waldron, K.J., "Force Distribution in Closed Kinematics Chains," IEEE J. ROBOTICS AND AUTOMATION, Vol 4 No 6, 1988, pp 657-663.

Imagery for Man-Machine Interfaces

906C0020 Tokyo INTELLIGENT FA SYMPOSIUM in Japanese 19 Jul 89 pp 55-56

[Article by Koshiro Sakai, Department of Mechanical Engineering, Yamaguchi University, Ube, Yamaguchi 755, Japan: "D1 Use of Images (Graphics) in Man-Machine Interfaces"]

[Text] In daily life, a human often applies imagery in understanding, thinking, and reasoning. For a computer or an interface to cooperate with a human operator, even simple figures can assist mutual understanding between the operator and the computer. For this purpose, the computer has to try to share images with the operator through monitoring the objective manufacturing process with the operator. The essential part of this procedure is "experiencing."

Introduction

Images play an important part in understanding and thinking. Our daily experiences show that they are very effective especially for basic-level reasoning and judgment. Therefore, if an image can be used well in a man-machine interface, it is possible to find a method to cope with the situation that has arisen as the interface and the man share an idea. To image something in the head, express it as a drawing, and show it to someone is particularly important in sharing an idea with that person. An image not only helps understanding, but it also works effectively in discovering how one person's idea differs from that of another. Here, we shall look at graphics (contours homomorphic to circles) as individual elements forming such images.

Making Images That Can Be Synchronized

To be able to show on display an image in which an interface can be synchronized with the party with whom one wishes to have a dialogue (to be referred to hereafter as "worker"), it is necessary to share experiences with the worker. Specifically, so that the interface can ensure mutual understanding with the worker, the image or display must convince the worker. Sharing experiences with the worker makes it possible for the two to have the same image of what happened. "Localization" playing a basic role in handling images in this article is described in a separate article for this lecture meeting.[1] Images are basically ambiguous. An image has a certain tolerance not exceeding the limits of one's past experience and is, therefore, acceptable if it is within those limits. If images are used as is, probably nothing else is acceptable. The limits of tolerance can be expanded or changed by study (instruction by the worker or the further accumulation of experiences). The accumulation of experiences as a row of experiences is conceived for the same graphic experienced, a "car," for example. In other words, a row of experiences is a row of an identical idea (pattern), such as "car," arranged according to a certain sequence. When memorizing a pattern, not the graphic itself but the results obtained by local linearization according to the abovementioned "localization" are memorized. As stated below on the procedure, this is a kind of feature extraction and only the features are memorized. (In the case of a human, however, there are some cautionary points in utilizing the form of interface, such as the fact[2] that the same graphic cannot be fully recognized depending on the direction it faces.) The "car" shown in Figure 1 can be divided into eight parts: U_i, $U_i \cap U_{i+1} \neq \phi$, $i = 1, \cdots, 8$, (provided that $i+1 = 1$ if $i=9$). These U_i's have a local coordinate system V_i on either the x-axis or the y-axis of the xy coordinate system. ($p(U_{ix}) = {}_Vi$, p is a coordinate map.) k_i, inclination of tangent, at each point on this V_i does not greatly vary on V_i, depending on how U_i is taken. Therefore, kbi can be represented by the value at a certain point of voltage$_i$. k_i, $i=1, \cdots, 8$ are arranged in this sequence and memorized as a visual experience. k_i is to be uniformly expressed by θ_i, a value replaced with an angle of inclination and measured counterclockwise with the x-axis (horizontal) as the standard. Geometrical features are extracted for adjoining domains i and i+1 by checking with all adjoining sets to see whether adjoining domains are linked by the "convex" relation or the "concave" relation, depending on whether $\theta_i - \theta_{i+1}$ is positive or negative (there can be no = 0). In the above, the length of each domain (segment) is not memorized. When reproducing a drawing, it is possible to reproduce it not necessarily as a straight segment but show it as a curve incorporating some nonlinearity and, in these respects, it is topological. If the "convex" and the "concave" are expressed by, respectively, 1 and 0, the car in the drawing, for example, belongs in the category of 10110111. (In the case of a triangle as the simplest example of graphic, the category is 111.) Further, the same category: 10110111 includes such concepts as ship and building. In these instances with a plural number of possibilities, the possibilities can be discerned through experiences (namely, by this method) or sometimes by knowing the context. If a definite contour can be extracted as a definite image based on experiences thus accumulated, this is f, response from the row of experiences for each divided portion to the real number. In the case of a "car," the graphic and j are memorized as showing, respectively, $a_j = (\theta_1, \theta_2, \cdots, \theta_8)_j$ and the j-th

experience. $f: X^* \rightarrow R^8$, using X^* for the space composed of rows of experiences (a_i). Specifically, what f is like depends on the norm of (subjective) evaluation that is to be used. As stated above, it is necessary for the worker and the interface to share the same experience.

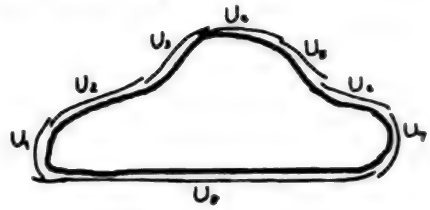

Figure 1.

Figure 2. Examples of Concepts Belonging to Category 10110111 and Identified by Accumulation of Experiences (Car, Ship, and Building)

References

1. Sakai, "On Human Procedure in Processing State Control," Published in this proceeding.

2. Rock, I., "The Logic of Perception," MIT, 1983, p 48.

Texture Analysis by Incoherent Optical Filter

906C0020 Tokyo INTELLIGENT FA SYMPOSIUM in Japanese 19 Jul 89 pp 57-58

[Article by Yoji Marutani, Osaka Prefectural Industrial Research Institute: "D2 Texture Analysis Using Incoherent Optical Filter"]

[Text] An optical-digital hybrid system is proposed for the texture analysis of images. Directional low-pass filtering is performed using an incoherent optical system. The output image of the system is then processed digitally to extract local features such as area and number of particles. These processes are repeated for appropriate directions. Finally, the features of each local area is examined and resembling areas are combined to construct the map of texture. This paper reports the principle of operation and an example of the experiments.

1. Introduction

One of the image processing methods available is texture analysis from the directivity of the distribution of concentrations by means of a concurrent

queue. It enables the uniformity and contrast of the distribution of concentrations to be determined separately by directions. But the processing to find a concurrent queue takes immense time. Meanwhile, space filtering can be done instantaneously by a simple lens system if an incoherent correlational optical system is used.[1] So, time taken by texture analysis can possibly be shortened. Here, I propose a formula for conducting texture analysis by digitally processing images whose directional components have been extracted by an optical space filter.

2. Composition and Principle of Operation

If, in the optical system in Figure 1, f(u,v) is the light intensity distribution on the input face, g(x,y), light intensity distribution of the image on the image formation face of the lens, L, can be shown by the following expression:

$$g(x,y) = \iint_{-\infty}^{\infty} f(u,v)\,m(u-x,v-y)\,dudv \tag{1}$$

Here, m(x,y) is the Fourier transformation of M(s,t), mask put on the lens face, and shown as

$$m(x,y) = k\iint m(s,t)\,e^{-jk(sx+ty)}\,dsdt \tag{2}$$

(K,k: constants determined by optical system)

Therefore, if M is a rectangle as in Figure 2(a),m is as shown in (b). So, the optical system in Figure 1 is a filter restricting spatial frequency components in a direction at right angle to the longer side of the rectangle.

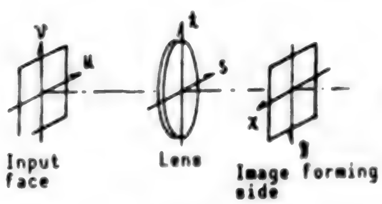

Figure 1.

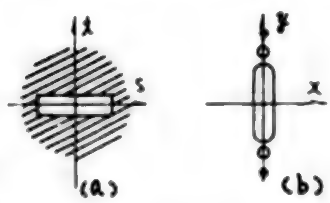

Figure 2.

Figure 3 is the flowchart of digital image processing after the image pickup of g(x,y). First, the direction of the mask is set at a certain angle θ and for binary terms. Then, divide into blocks of suitable size and compute area s and number of independent graphics p in each block. These values are used as block characteristic quantities $s(m,n,\theta)$ and $p(m,n,\theta)$. These measurements are repeated for the necessary number of times using different mask angles. Then, these characteristic quantities are compared between blocks, similar blocks are integrated together and the whole picture is regionally divided by textures.

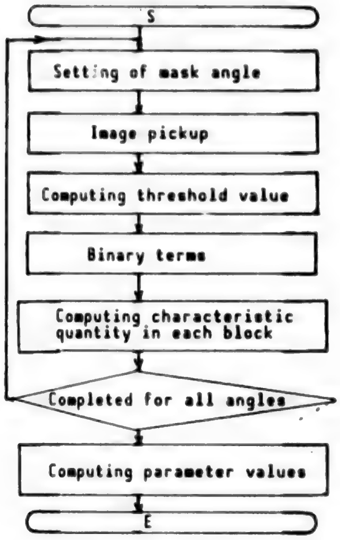

Figure 3.

3. Test Results

Figure 4 is an example of test results. The image in (a) of the figure is divided into 64 x 64 pixels. The number of blocks is 8 x 7. (b) and (c) are block characteristic quantities shown when the filter angle is, respectively, 0 and 90.

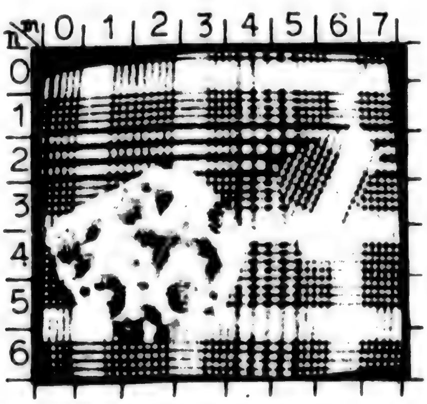

(a)

n\m	0	1	2	3	4	5	6	7
0	62 7	79 3	69 4	82 3	73 4	70 6	82 4	70 8
1	54 11	60 4	69 20	75 6	65 14	61 13	74 13	72 22
2	54 5	67 9	76 6	73 3	58 7	58 7	80 4	81 8
3	62 4	55 1	71 3	90 4	81 6	80 3	92 3	83 17
4	78 9	72 2	80 4	94 2	87 7	78 11	93 4	74 27
5	63 5	80 4	89 4	97 3	80 6	85 6	92 4	84 14
6	[illegible] 16	63 16	65 23	74 11	62 13	60 21	83 10	70 27

(b)

n\m	0	1	2	3	4	5	6	7
0	77 2	83 2	83 3	83 3	78 3	77 3	78 3	78 3
1	51 [illegible]	54 [illegible]	52 5	57 5	56 5	53 5	58 4	58 4
2	47 4	54 3	64 3	59 2	49 3	60 11	87 14	77 5
3	79 3	69 2	69 2	95 2	78 3	82 7	[illegible] 8	74 5
4	64 7	95 3	98 4	91 3	79 1	60 4	77 4	63 5
5	62 3	86 1	88 4	94 1	83 2	82 3	80 3	79 3
6	51 5	54 5	54 5	56 6	50 6	51 5	58 5	56 5

(c)

n\m	0	1	2	3	4	5	6	7
0	A	0	3	1	1	2	1	3
1	3	5	F	3	F	F	7	F
2	3	F	3	4	7	3	9	3
3	1	0	0	0	3	1	1	B
4	3	1	1	1	A	F	5	F
5	3	8	1	8	A	3	5	B
6	F	F	F	3	7	F	7	F

(d)

Figure 4.

Here the shape parameters of blocks are shown by the following four bits:

$$\alpha = 0(0,5<p(m,n,90)/p(m,n,0)<2,), = 1 \text{ (otherwise)} \tag{3}$$

$$\beta = 0(0.9<s(m,n,90)/s(m,n,0)<1.1), = 1 \text{ (otherwise)} \tag{4}$$

$$\gamma = 0(p(m,n,0)<5), = 1 \text{ (otherwise)} \tag{5}$$

$$\delta = 0(p(m,n,90)<3), = 1 \text{ (otherwise)} \tag{6}$$

Figure 4(d) shows the results as hexadecimal numbers by arranging them in the order of (α β γ δ). Therefore, numerical proximity does not necessarily mean morphologic proximity.

It can be seen from (a) and (d) that similar domains have similar parameter values.

4. Postscript

In the test, the mask was turned θ by θ because only one set of optical space filters was used. But processing can be speeded up by paralleling as in Figure 5.

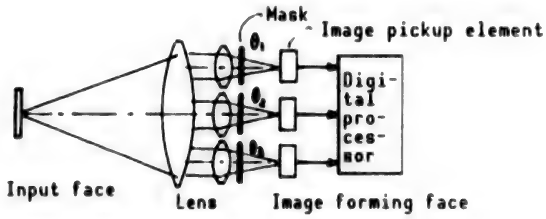

Figure 5.

Regarding the combination of block characteristic quantities, automatic learning methods, such as the neuro-network, may possibly be used.

Fixed block division was used this time because of the inadequate memory capacity of the equipment but more accurate domain division is possible if variable block size or pixel-by-pixel locomotion is used.

References

1. Zitahama, et al., JOURNAL OF PAPERS OF ELECTRONIC COMMUNICATIONS SOCIETY, 53C-10, 1970, pp 683-690.

Guiding Autonomous Robots by Cognitive Map

906C0020 Tokyo INTELLIGENT FA SYMPOSIUM in Japanese 19 Jul 89 pp 65-66

[Article by M. Yamamoto, K. Hemmi, K. Kamei, and K. Inoue, Faculty of Science and Engineering, Ritsumeikan University: "D5 Cognitive Map Based Navigation of Autonomous Robots"]

[Text] **Abstract** A human can find his own route from starting point to destination, by means of knowledge about some positions of some objects and some paths. And then, he makes use of a cognitive map, which includes the relationship between some characteristic points and the area. We represent that a cognitive map applies to a map-based navigation method for an autonomous robot.

In this report, the construction method of the indoor map and the navigation method are described.

1. Introduction

A human can find a route to a desired destination using his knowledge about the spatial arrangement of objects and paths. In doing so, he uses a cognitive map composed by positioning landmarks and clues to the locality.

There are various methods to guide autonomous mobile robots but the authors are attempting to guide a robot with a visual sensor, using this cognitive map for guidance under known environments.[1]

In this report, we will describe how to compose a map indoors and how to indicate a route by a cognitive map.

2. Composition of Maps

2.1 Cognitive Map

When a human shows a route by language, he indicates it as follows:

> "Go straight along the corridor and turn right at the first T junction; the first door is the door to the teachers' room."

This is composed of a mark to serve as a subgoal and instructions necessary to reach the target and takes the form of guiding to the destination by setting a plural number of subgoals. This is a kind of cognitive map called a road map.[2] It shows a route by words denoting a specific place and does not include two-dimensional information.

Guiding a robot by such a road map has advantages that include the following:

(1) Since it does not include distance information, it is unnecessary to measure distance traveled and consider errors in this measurement.

(2) By setting subgoal marks suitable for image processing, it is possible to reduce processing time.

2.2 How To Compose a Map

To use a road map to guide a robot, there must be arms which are systematically placed on the map. In this study, no artificial landmarks for the robot are used. Instead, the following indoor objects are used as marks.

(1) Doors

(2) Corners, intersections, and T junctions.

Information concerning doors is necessary for locomotion from room to room. Also, directions change at a corner and may change at an intersection or a T junction. So, information on these points must be shown on the map.

These are composed of straight lines and are therefore expected to be relatively easy to extract from images.

A map is composed of a graph noded with characteristic points which are marks in 1) and 2). Figure 1 is an example.

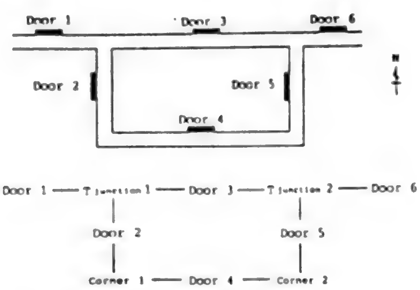

Figure 1. Indoor Environment and Map

At such branch joints as intersections and T junctions, the directions of adjacent characteristic points are indicated in terms of east, west, north, and south. Figure 2 is an example of data on a T junction.

T junction 1	
North	
South	Door 2
East	Door 3
West	Door 1

Figure 2. Data on T Junction

When preparing a route, these data are only used to decide whether to go straight or turn right or left. So, precise agreement with actual direction is not always necessary. For a corner involving right or left turn, indication must be made similarly to a branch point.

3. Preparation of Routes

When the characteristic points that are to be the start and the goal and the general direction of the goal are inputted, the robot makes route searching and checks on the characteristic points to be passed through before reaching the goal. If it is an unforked road, the robot proceeds toward the goal but in the case of a branch point, it takes the road running in the direction of the goal and, if it turns out to be a dead-end, the robot returns to the branch point and checks for another road. This is repeated until the robot reaches the goal. It forms a route by reading from the map the travel commands for reaching subgoals that are characteristic points. A travel command is judged by the type of the present characteristic point as follows:

(1) Doors

If the present place is a door, the travel command is always "go straight."

(2) Corners, T junctions, and intersections

If the present place is a branch point: a corner, a T junction or an intersection, judgment as to whether to go straight or turn right or left is made by referring to the branch point data in Figure 2.

Indication of the route to the goal thus prepared takes the same form as the road map. For example, route indication with Door 1 as the start and Door 2 as the goal is given by Figure 3.

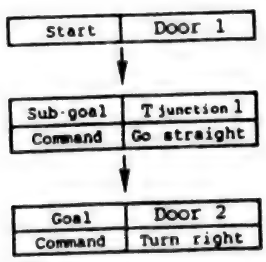

Figure 3. Example of Route Indication

4. Conclusion

We have seen how to compose an indoor map with a graph using characteristic points as nodes and how to guide, using this map. In the future, we will study how to process if characteristic points cannot be recognized and apply the results to practical traveling.

References

1. Yamamoto, Hemmi, Kamei, and Inoue, "How To Compose Maps for Autonomous Mobile Robots," Collection of papers announced in 33rd Research Announcement Lecture Meeting of System Control Information Society, 1989, pp 117-118.

2. Anderson, J.R., "Outline of Cognitive Psychology" [Nirchi Shinrigaku Gairon], Seishi Shobo, pp 90-97.

High-Speed Noncircular Machining NC-Lathe for Engine Pistons

906C0020 Tokyo INTELLIGENT FA SYMPOSIUM in Japanese 19 Jul 89 pp 101-102

[Article by Toshiro Higuchi, Institute of Industrial Science, University of Tokyo; Tomomi Yamaguchi, Advanced Software Technology and Mechatronics Research Institute of Kyoto; and Minoru Tanaka, Izumi Automotive Industry Co., Ltd.: "F5 Development of a High-Speed Noncircular Machining NC-Lathe for Cutting a Piston-Head of a Reciprocating Engine"]

[Text] **Abstract** This paper presents a high-speed noncircular NC-lathe for cutting a piston-head of a reciprocating engine. The positioning of a cutting tool is necessary for noncircular machining. This positioning mechanism needs high-frequency response and high power. So we have applied the mechanism by the electromagnetic force to it, and have developed the high-speed noncircular machining NC-lathe. In this machining, a piston-head of a reciprocating engine can be machined in the accuracy of 2 μm at 3000 rpm. This machining performance is superior to any other conventional machining lathes.

1. Introduction

The development of high-speed noncircular machining NC-lathe especially for cutting piston-heads for a reciprocating engine has progressed in recent years. This machining requires a cutting tool positioning mechanism combining high-speed response and high output and the authors have developed a highly efficient noncircular machining NC-lathe, using an electrohydraulic servomechanism for this positioning.[1,2] However, hydraulic driving involves practical problems, such as large equipment and the cumbersome maintenance of oil, etc.

This method describes the development of the piston machining high-speed NC-lathe with a high-speed positioning mechanism driven by the electromagnetic suction force by the electromagnet proposed as a cutting tool positioning mechanism,[3,4] taking its practical aspects into consideration, and the machining performance of this lathe.

2. Outline of Piston Machining NC-Lathe

Figure 1 shows the outline of the lathe developed. This lathe detects the angle of rotation of the main shaft by a 512 pulse/rev. encoder attached to

the main shaft, outputs input data put into the computer in advance successively to the positioning control system by detecting signals from the encoder and thus makes positioning and machining. The lathe is so conditioned that one bit in the S/A and A/D converters may be 0.12 μm by the displacement of the cutting tool. Figure 2 shows the outline of the positioning device. In it, the cutting tool is attached to the tip of the shaft. In this device, plate springs are used as springs to be attached. These plate springs not only give the effect of spring attachment[4] but also guide the moving parts. In contact support guiding mechanisms, such as ball splines, breakdown, abrasion, and life become problems but this device has solved these problems by using plate springs.

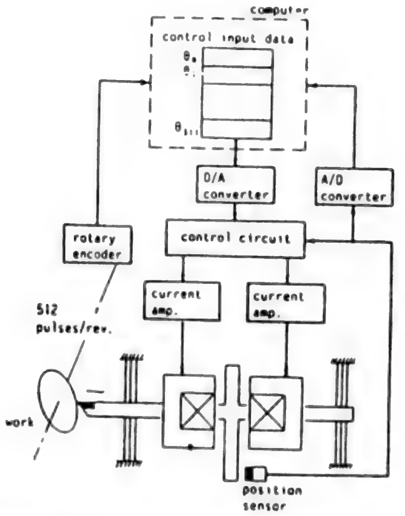

Figure 1. Outline of Noncircular NC Lathe

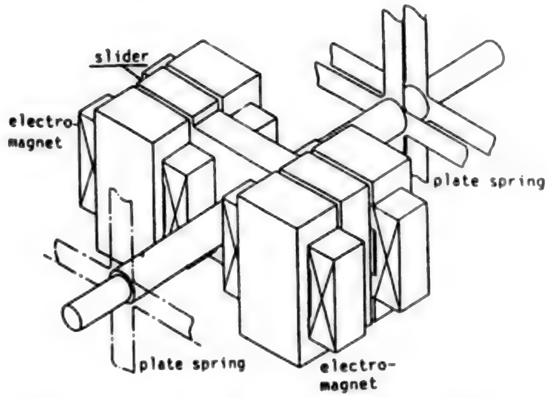

Figure 2. Outline of Positioning Mechanism

As a method to control cutting tool positioning, we used repetitive control combined with inverse transfer function compensation.[5]

3. Machining Performance

We checked for machining performance by conducting noncircular machining under the following processing conditions:

The processing target shapes used were the shapes of pistons with the sectional shapes of $f(\theta) = 45 + 0.125 \cos 2\theta$[mm] and $f(\theta) = 45 + 0.04 \cos 2\theta$[mm]. These are near ellipses and expressed as a ϕ0.5 ellipse and a ϕ0.16 ellipse in view of the fact that generally, an ellipse with a major axis-minor axis difference of x mm is expressed as a ϕx ellipse. The material to be cut was an AC8A bar (ϕ90x120): Al alloy often used as a piston material. The number of revolutions of the main shaft was 3000 rpm, the feed was 0.12 mm/rev., the depths of cut were 0.15 mm (ϕ0.5 ellipse) and 0.1 mm (ϕ0.16 ellipse) and the cutting tool material was compact (diamond).

Figure 3 shows the results of measurement of shapes attained by processing the ϕ0.5 and ϕ0.16 ellipses. From it, one can see that both shapes can be

processed with accuracies of less than 2 μm by correcting input data, using repetitive control combined with inverse transfer function compensation.[5]

(a) ϕ0.5 ellipse (b) ϕ0.16 ellipse

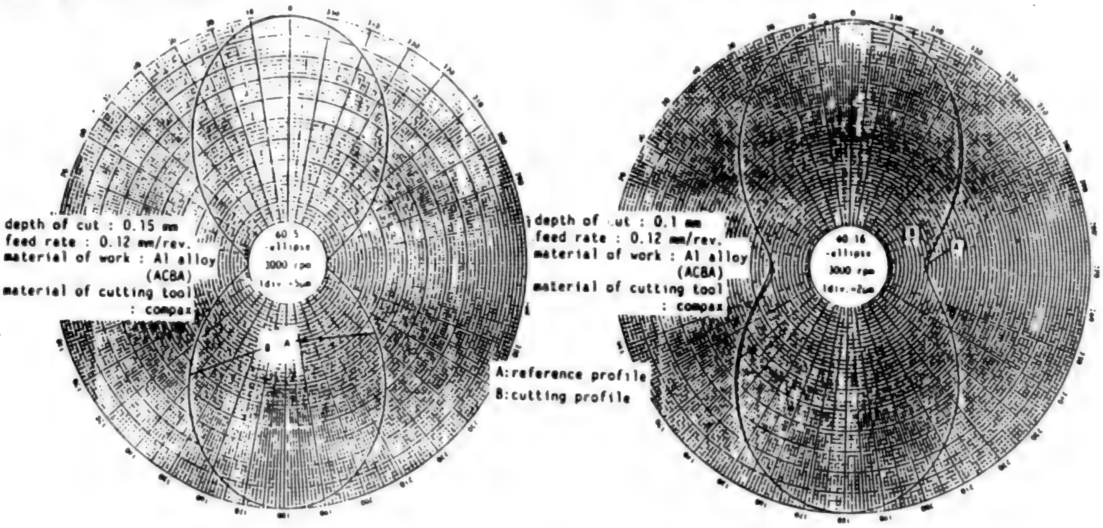

Figure 3. Measurement of Processed Shapes

4. Conclusion

We have developed a piston-cutting high-speed noncircular machining NC-lathe using a high-speed processing mechanism by electromagnetic suction force by an electromagnet and confirmed that it can process with an accuracy of 2 μm at 3000 rpm. This lathe is a useful processing machine because it can not only process but its positioning mechanism is simple and compact.

References

1. Higuchi and Yamaguchi, JOURNAL OF PRECISION INDUSTRY SOCIETY, Vol 54 No 1, p 145.

2. Higuchi, Yamaguchi, et al., 1988 Spring Precision Industry Society, p 65.

3. Higuchi and Yamaguchi, 1987 Autumn Precision Industry Society, p 327.

4. Ibid., 1988 Spring Precision Industry Society, p 917.

5. Ibid., SYSTEM AND CONTROL, Vol 30 No 8, p 503.

FY90 Science & Technology Budget Proposals Reported

90FE0098A Tokyo PUROMETEUSU in Japanese 1 Mar 90 pp 66-72

[Text] FY90 Science & Technology Budget Proposal

About 1.9 Trillion Yen, a 5.7 Percent Increase for the Promotion of an Abundant and Creative Science & Technology

- Coordination Division, Science & Technology Policy Bureau, Science & Technology Agency

The Science and Technology Agency [STA] has the position of comprehensively furthering science and technology policy. The coordination of policy execution among the related government ministries and agencies is one of its major tasks. At this time, we have put together an outline of the government's science and technology budget proposal.

The government, for the purpose of promoting science and technology, passed at a Cabinet conference in March 1986, a proposal entitled "Science and Technology Policy Outline." The proposal, while giving consideration to the harmonious development of science and technology with mankind and society and the development of a science and technology that focused on internationalism, mainly emphasized the promotion of an abundant and creative science and technology.

STA is responsible for comprehensively advancing policy on science and technology for the purpose of promoting science and technology. One of its major tasks is to comprehensively coordinate the execution of science and technology policy among the various government ministries and agencies. Below is an outline of its FY90 science and technology budget proposal.

A Science and Technology Budget Spread Over All Government Offices

The science and technology budget is shown in Table 1, and consists of the expenses for promoting science and technology and other research related expenses in the general account, along with expenses placed in the special account. (Note)

Science and Technology Expenses in the General Account

- Science and Technology Promotion Expenses

One of the major expense areas in the general account consists of national laboratory research organization expenses, various subsidies, and government contributions.

- Other Research Related Expenses

These consist of research related expenses other than those promoting science and technology and accounted for in the general account (energy policy expenses, education promotion subsidies, economic cooperation expenses, small and medium firm policy expenses, and things included in other expense items).

Science and Technology Expenses in the Special Account

These consist of research related expenses in the special account such as the public secondary school special account; the electric power source development and furtherance policy special account; the coal and oil, as well as oil substitute energy, policy special account; and the industrial investment special account.

Total is 1,919,600,000 Yen and Focus is on the General Account Budget

The proposed FY90 science and technology budget is 1.9196 trillion yen. If we compare it to last year, we find that the first proposed budget last year was 1.8156 trillion yen. When compared with that 1.8156 trillion yen of last year, it has a growth factor of an overall increase of 104 billion yen. When compared with the budget this year, it represents an increase of 5.7 percent. Out of this, the general account budget portion is 903.4 billion yen. When compared with last year's first budget amount of 862.5 billion yen, it grew at 4.7 percent or an increase of 40.9 billion yen, or a 4.7 percent increase. Moreover, the special account portion is 1.0162 trillion yen. When compared to last year's initial budget amount of 953.2 billion yen, it is an increase of 63 billion yen, or 6.6 percent. Incidentally, science and technology promotion expenses in the general account budget is 475.5 billion yen. Compared with last year's initial budget of 448 billion yen, it is an increase of 27.5 billion yen, or 6.1 percent.

Table 2 shows that the general ways and means in the FY90 budget account represents an increase over last year's expenses of 3.8 percent. The promotion of science and technology is said to be considered a focal concern.

Incidentally, Tables 3 and 4 illustrate the breakdown of the FY90 science and technology budget proposal by government ministry and agency, while Figure 1 illustrates the changes in science and technology related budgets.

Table 1. Composition of the Science and Technology Budget

- Science and Technology Budget
  - Science and Technology Expenses Within the General Account
    - Science and Technology Promotion Expenses
    - Other Research-Related Expenses
  - Science and Technology Expenses Within the Special Accounts

Figure 1. Changes in the Science and Technology Budget (Unit: One hundred million yen)

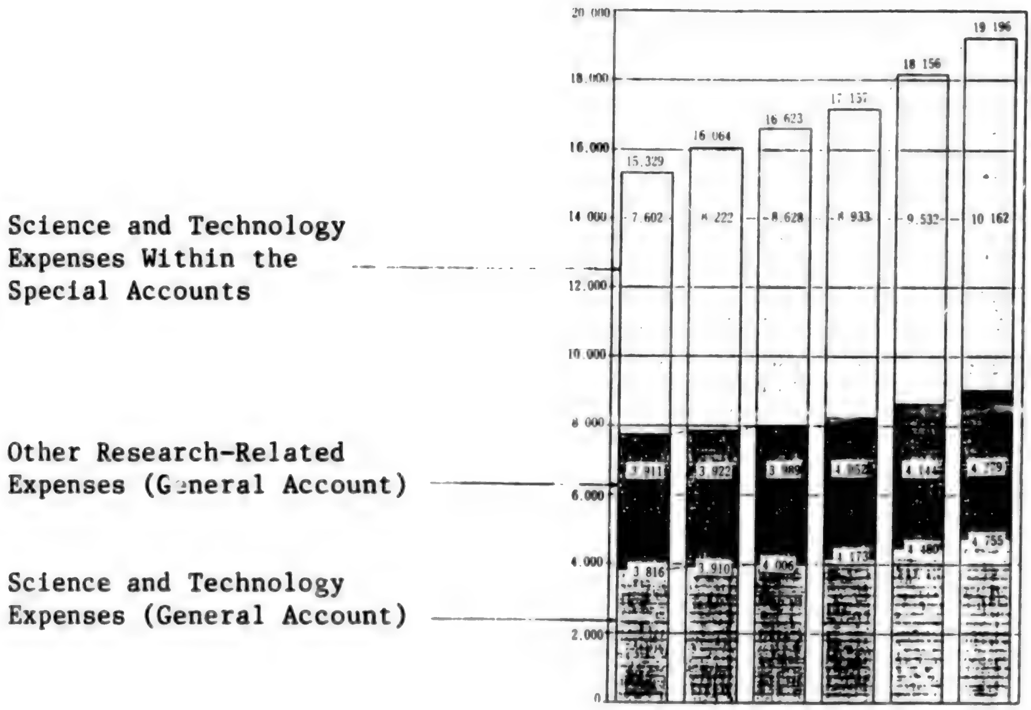

[Figure 1 continued on following page]

[Figure 1 continued]

Fiscal Year	1985	1986	1987	1988	1989	1990
Science and technology promotion expenses	(1.3) 3,816	(2.5) 3,910	(2.5) 4,006	(4.2) 4,173	(7.4) 4,480	(6.1) 4,755
Other research-related expenses within the general account	(1.1) 3,911	(0.5) 3,922	(1.4) 3,989	(1.6) 4,052	(2.3) 4,144	(3.3) 4,279
Science and technology expenses within the general account	(1.2) 7,727	(1.5) 7,842	(2.0) 7,995	(2.9) 8,225	(4.9) 8,624	(4.7) 9,034
Science and technology expenses within the special accounts	(5.5) 7,602	(8.2) 8,222	(4.9) 8,628	(3.5) 8,933	(6.9) 9,532	(6.6) 10,162
Total science and technology budget	(3.3) 15,329	(4.8) 16,064	(3.5) 16,623	(3.2) 17,157	(5.8) 18,156	(5.7) 19,196

The percentage of increase or decrease vis-a-vis the previous year is in brackets.

Table 2. Comprehensive Table on the FY90 Science and Technology Budget (Unit: One Million Yen)

unit: 100 million

	Category / Fiscal Year	1989 budget	1990 proposed budget	increase decrease
	Science and technology promotion expenses	448,032	475,460	6.1
	Other research-related expenses	414,418	427,921	3.3
	Science and technology expenses within the general account	862,451	903,381	4.7
	Science and technology expenses within the special accounts	953,166	1,016,222	6.6
	Total science and technology budget	1,815,616	1,919,603	5.7
REFERENCE	Total general account	60,414,194	66,236,791	9.6
REFERENCE	General expenditures out of the general account	34,080,487	35,373,114	3.8

(Notes)

1. General expenditures consist of all expenses from the total general account except for government bonds, local transfer tax subsidies, and transfers to the Industrial Investment Special Account.
2. This table is an STA estimate.
3. The additions in each column and the total amounts are rounded off to the nearest whole and therefore do not match.

Table 3. Comprehensive Table of the FY90 Science and Technology Budgets of Individual Government Offices (as Estimated by STA)

Item / Government Ministry or Agency	Science and Technology Promotion Expenses		Other Research-Related Expenses Within the General Account		Science and Technology Expenses Within the General Account		Science and Technology Expenses Within the Special Accounts		Total Science and Technology Budget	
	A	Percentage Increase or Decrease vis-a-vis the Previous Fiscal Year	B	Percentage Increase or Decrease vis-a-vis the Previous Fiscal Year	C=A+B	Percentage Increase or Decrease vis-a-vis the Previous Fiscal Year	D	Percentage Increase or Decrease vis-a-vis the Previous Fiscal Year	C+D	Percentage Increase or Decrease vis-a-vis the Previous Fiscal Year
Diet	533	0.0	-	-	533	0.0	-	-	533	0.0
Science Council of Japan [SCJ]	-	-	951	9.7	951	9.7	-	-	951	9.7
National Police Agency [NPA]	1,055	3.4	-	-	1,055	3.4	-	-	1,055	3.4
Hokkaido Development Agency [HDA]	149	1.4	-	-	149	1.4	-	-	149	1.4
Japan Defense Agency [JDA]	-	-	104,268	12.0	104,268	12.0	-	-	104,268	12.0
Economic Planning Agency [EPA]	809	5.8	-	-	809	5.8	-	-	809	5.8
STA	204,905	8.2	164,933	△ 0.7	369,838	4.1	124,937	12.4	494,775	6.0
Environment Agency [EA]	9,217	16.9	-	-	9,217	16.9	-	-	9,217	16.9
Ministry of Justice [MOJ]	939	7.8	-	-	939	7.8	-	-	939	7.8
Ministry of Foreign Affairs [MFA]	-	-	7,095	10.7	7,095	10.7	-	-	7,095	10.7
Ministry of Finance [MOF]	358	2.7	-	-	358	2.7	730	△ 1.1	1,087	0.1
Ministry of Education [MOE]	74,673	9.1	129,907	1.2	204,580	4.0	689,721	4.9	894,301	4.7
Ministry of Health and Welfare [MHW]	38,831	6.8	1,319	13.5	40,150	7.0	10,092	2.3	51,242	5.9

[Table continued]

Ministry of Agriculture, Forestry, and Fisheries [MAFF]	64,164	2.9	2,544	11.2	66,707	3.2	3,300	△ 2.9	70,007	2.9
Ministry of International Trade and Industry [MITI]	55,580	△ 0.4	12,912	△ 5.3	68,492	△1.3	181,340	10.4	249,832	6.9
Ministry of Transportation [MOT]	13,060	△ 1.2	3,311	53.2	16,371	6.4	1,039	13.3	17,410	6.8
Ministry of Posts and Telecommunications [MPT]	4,468	2.9	189	79.8	4,657	4.7	26,543	0.5	31,199	1.1
Ministry of Labor [MOL]	630	3.0	38	5583.6	668	9.1	3,522	△11.0	4,190	△ 8.1
Ministry of Construction [MOC]	5,525	2.8	454	45.3	5,979	5.1	-	-	5,979	5.1
Ministry of Home Affairs [MHA]	565	1.8	-	-	565	1.8	-	-	565	1.8
Total	475,460	6.1	427,921	3.3	903,381	4.7	1,016,222	6.6	1,919,603	5.7

(Notes)

1. With regard to the science and technology budget within the Industrial Investments Special Account, which is under the jurisdiction of MOF, the 3.8 billion yen expenses of the Japan Science and Technology Information Center are in STA's account, the 2.3 billion yen expenses related to investments in experimental research into pharmaceutical technology within the Expense Fund to Promote Research into Relief from Damage Caused by the Secondary Effects of Pharmaceutical Products are in MHW's account, the 3.3 billion yen expenses related to the Organization for the Promotion of Specified Organic Industrial Technology Research are in MAFF's account, the 2.2 billion yen expenses related to the New Energy and Industrial Technology Development Organization are in MITI's account, and, along with these, the 26 billion yen expenses for the Base Technology Research Advancement Center are accounted for both in MITI's and MPT's accounts. (Incidentally, the total is not redundant between the two accounts.)

2. The table is an STA estimate.

3. The numbers added up each column and the totals do not match because of rounding off to the nearest whole.

Table 4. Major FY90 Science and Technology Budget Items by Government Office (Unit: One Million Yen)

Government Office and Item(s)	FY89 Budget	FY90 Budget	Remarks
NPA Scientific Police Research Institute expenses	1,020	1,055	Two special research problems (one of which is research on distinguishing individuals by their features by means of applying new high speed imagery conversion devices)
HDA Development Land Research Institute expenses	147	149	
JDA Technology Research Office expenses, etc.	93,068	104,268	Starting to develop shipboard fire direction systems
STA Contribution to international society through science and technology	47,407	62,914	
-Advancement of science and technology contributing to the resolution of global environmental problems	2,762	5,291	-Reorganization of the Disaster Prevention Science and Technology Research Institute (hypothetical name) of the National Disaster Prevention Science and Technology Center -Specific global science and technology investigative research-311 (117)

[Table continued]

-Advancement of international cooperation and exchange	44,955	59,481	-Advancement of the Human Frontier Sciences Program-1,872 (1,456) -Furtherance of the international distribution of grey literature-150 (0)
Strengthening of creative and basic research	6,408	7,847	
-Strengthening of the research activities in national experimental research organizations	0	210	-Increase of per capita research expenses with all the government offices combined -Special science and technology researcher system-200 (0)
-Enlargement of the special basic science researcher system	106	426	
-Enlargement of the creative science and technology advancement system	6,302	7,211	-Starting four new tasks (fluid dynamics (hypothetical name), protein accumulation (hypothetical name), food information regulation (hypothetical name), and recognition connotation entities (hypothetical name))
Preparation of the base for science and technology promotion	11,279	12,365	
-Advancement of the regional development of research and development	311	928	-Regional development of frontier research-261 (0) -Creation of a regional current research system-200 (0) -Preparation of large optical radiation facility-2,801 (1,900)
-Preparation of base for research and development	10,968	11,437	-Furtherance of science and technology when transmitted-5,582 (6,935)

[Table continued]

Strengthening of the comprehensive advancement function of science and technology policy	10,693	10,837	
-Enlargement of science and technology promotion coordination expenses	10,000	10,200	
-Fulfillment of science and technology policy research	481	536	
-Advancement of publicity and education activities	112	102	
Advancement of research and development in leading edge and major science and technology fields	443,201	469,105	
-Advancement of atomic energy research and development uses safety measures	281,643	296,214	Fulfillment and strengthening of atomic energy safety measures-33,024 (31,003) Establishment of the nuclear fuel cycle-52,643 (50,532) Development of new power reactors and plutonium uses-89,126 (95,329) Advancement of leading edge projects-49,223 (47,597) Strengthening of policies to further the understanding and cooperation of the nation-24,556 (18,981)
-Advancement of space development uses	109,062	119,416	Development of the H-II rocket-37,799 (22,719) Development of man-made satellites-47,218 (30,295) Participation in the space station project-9,796 (2,997)

[Table continued]

-Advancement of marine development	10,573	9,864	Deep sea survey research-6,026 (0)
-Advancement of research and development of global science and technology	30,893	26,933	Research and development of global environment observation technology-22,813 (27,263) Analysis and research of various global-scale phenomena-1,338 (1,005)
-Advancement of research and development of physical materials science and technology	13,066	13,675	Advancement of superconductor materials research-3,460 (3,945)
-Promotion of life science	17,070	19,081	Advancement of cancer related research-9,234 (8,014)
-Advancement of other important comprehensive research	18,615	18,210	Aerospace technology related research-7,462 (7,914)
EA			
Environmental preservation comprehensive survey research promotion coordination expenses	175	175	
National organization pollution prevention experimental research expenses	2,283	1,928	93 tasks (26 new tasks among them) (all accounted for under EA)
Pollution prevention survey research expenses	869	1,015	Development of stratification and ozone layer observation equipment
Expenses for the comprehensive advancement of global environment research	0	1,200	
Experimental research organization expenses (two organizations)	4,556	4,899	Reorganization of the National Environmental Research Institute (hypothetical name) of the National Pollution Research Institute

[Table continued]

MFA			
International Atomic Energy Agency share	2,616	2,956	
OECD Atomic Energy Agency share	191	200	
MOF			
Brewing Laboratory expenses	348	358	Two special research tasks (Within these, "Research Concerning the Structure and Function of Brewing Related Microbes")
Printing Bureau Research Institute expenses	738	730	
MOE			
Scientific research expenses subsidy	52,600	55,800	
Science Council of Japan subsidy	5,568	6,148	
Public and private university research related subsidies	128,366	129,907	
National university research-related expenses	657,517	689,721	
MHW			
Scientific experimental research subsidy	17,825	18,844	Specified disease treatment research expenses-18,149 (17,175)
Health and welfare scientific research subsidy	5,464	6,467	Health policy survey research-50 (0)

[Table continued]

Investment enterprise expenses for experimental research with pharmaceuticals from the Fund to Promote Research into Relief from Damage Caused by the Secondary Effects of Pharmaceutical Products	2,400	2,300	Rheumatism survey research-100 (0) (Special licensed organization, Industrial Investment Special Account)
Experimental research organization expenses (11 organizations)	15,125	15,706	Eight special research tasks (three new tasks among these)
(Reference: Anti-cancer 10-year comprehensive strategy expenses)	1,639	1,836	Reorganization of the National Medical and Hospital Management Research Institute (hypothetical name) of the Hospital Management Research Institute
MAFF			
Experimental research organizations (29 organizations)	57,455	59,221	
Comprehensive development research	722	742	Three tasks
Large-scale special limit research	1,300	1,302	Three tasks
General special limit research	322	453	Five tasks (Among are two new tasks, including "The Development of Predictive Technology and the Vital Analysis of Agriculture, Forestry, and Fisheries Ecology Accompanying Global Environmental Changes")
Development of advanced biotechnology	1,509	1,565	Six tasks
Tropical agricultural research advancement enterprise	624	672	
Specified Organic			

[Table continued]

Industrial Technology Research Promotion Organization expenses	3,400	3,300	(Special licensed organization, Industrial Investment Special Account)
MITI			
Large-scale industrial technology research and development expenses	12,993	13,161	11 tasks (Two new tasks among them: "Advanced Function Creation Processing Technology" and "Human Perception Measurement Applied Technology")
New energy technology research and development expenses	27,139	27,475	
Energy conservation technology research and development expenses	10,305	11,120	
Next generation industrial base technology research and development	6,836	7,463	New "New Software Structuralized Model"
Experimental research organizations (16 organizations)	40,248	40,849	Global environment technology research and development-165 (97)
Electronic calculating device basic technology development consignment expenses	3,772	3,465	
Medical and welfare equipment technology research and development expenses	659	671	10 tasks (Three new tasks among them: "Non-invading Continuous Blood Sugar Value Measurement System," "Digital Hearing Aid," "Aging Society Support Equipment")
Human Frontier Sciences Program advancement	932	1,337	
Base Technology Research Promotion Center expenses	26,000	26,000	(Special licensed organization, Industrial Investment Special Account)

[Table continued]

Outlays and aid (general account) to the New Energy and Industrial Technology Comprehensive Development Organization	7,675	6,544	Partial re-addition of large-scale industrial technology research and development, next generation industrial base technology research and development, and medical and welfare equipment research and development
Outlays (special account) to above	2,200	2,200	Research base preparation enterprise (Outlays, Industrial Investment Special Account)
Founding of Global Environmental Industrial Technology Research Institute (hypothetical name)	290	6,010	(Foundation, oil in special account, and some in general account)
MOT			
Experimental research organization expenses (five organizations)	8,308	8,595	15 special research tasks (Four new tasks among them)
Research and development of transportation technology	142	136	Three tasks (One new task among them: "Development Research of a New Traffic System in Waterfront Areas")
Geostationary meteorological satellite launching consignment expenses	3,481	3,272	
Geostationary meteorological satellite operations expenses	2,251	2,130	
Railroad technology development subsidy	235	210	Three tasks
Magnetic levitation railroad technology development subsidy	900	2,017	
Next generation ship research and development subsidy	746	800	

[Table continued]

MPT			
Telecommunications Frontier research and development advancement	247	389	
Telecommunications Comprehensive Research Institute expenses	4,341	4,468	13 special research tasks (One new task among them: "Research of Measurement Technology of the Global Environment by Short Wave Millimeter Wave Band Electromagnetic Waves")
Postal Research Institute expenses	417	543	
Base Technology Research Promotion Center expenses	26,000	26,000	(Special licensed organization, Industrial Investment Special Account)
MOL			
Research and development of equipment to expand the areas of employment and ensure the safety and health of the elderly	0	118	Five tasks
Experimental research organization expenses (Two organizations)	2,706	2,432	Five special research tasks (Among these is one new task: "Research Concerning the Development of Scientific Evaluation Methods for Immunizations Against Employment Allergies")

[Table continued]

MOC			
Construction technology research and development expenses	709	733	Nine tasks (Two new tasks among them: "Development of new Operational Technology in Construction Enterprises")
Experimental research organization expenses (two organizations)	4,572	4,693	Seven special research tasks (One new task among them: "Joint Japan-U.S. Research on Earthquake Resistance Improvement Technology by Means of Hybrid Controls")
MHA			
Fire Defense Research Institute expenses	555	565	Eight special research tasks (Two new tasks are included among them: "Research Concerning the Nature of Fires in Special Space Used Underground" and "Research on the Risk Evaluation of Self-Reactive Substances.")

Note: The number in brackets in the remarks section is the FY89 budget amount.

Problems With Practical Use of High-Temperature Oxide Superconductors

906C7513A Tokyo KO ON CHODENDOTAI NO JITSUYOKA E NO TENBO in Japanese
17 Jan 90 pp 5-10

[Article by Keiichi Ogawa, National Research Institute for Metals]

[Text] 1. Preface

Problems to be resolved to put high-temperature oxide superconductors into practical use can be classified roughly into two major problems: application technology, with which ferromagnetic fields are involved in some forms, and electronics application-related technology. In the former case, the processing of superconducting materials into superconducting wires and high critical current density are the major subjects to be studied. In the latter case, the technology for processing superconducting materials into thin films, particularly, the low-temperature (600°C or lower) process is the major research subject. This paper first describes an atomic structure and an electron structure peculiar to high-temperature oxide superconductors. Then, on the basis of such structures, problems with high-temperature oxide superconductors are discussed. In other words, c-face orientation, anisotropy, pinning, and manufacture of thin films are highlighted in this paper.

2. Features of Microscopic Structure

(1) Structural Features

(i) CuO_2 Face

The following are the basic crystal structures of high-temperature oxide superconductors.

- $(La, Ba)_2CuO_4$
- $YBa_2Cu_3O_{6+x}$
- $Bi_2Sr_2Ca_{n-1}Cu_nO_x$ (n=1,2 ...)
- $(Nd, Ce)_2CuO_4$

These structures can be deemed to be tetragonal crystals (lattice constants a, c), or to have been slightly deformed from tetragonal crystals (for

example, orthorhombic crystals a~b, c, or a modulated structure that can be seen in Bi system). The size of an axis is about 3.8 Å in any system. This shows that the size of an axis is determined by CuO_2 faces that all high-temperature oxide superconductors contain. In other words, the bonding of Cu-O controls the size of an axis. In high-temperature oxide superconductors, the level of energy that each Cu and O ion valence electron possess is close to each other and, therefore, each wave function fully mixes with each other. However, such naive imaging of CuO_2 faces cannot explain the electrical characteristics of high-temperature superconductors, because from the initial stage, consideration must be given to strong correlations between carriers (see 2 (2)(i)).

(ii) Anisotropy:

CuO_2 faces are separated from each other by an oxide layer that does not contain copper. This is another feature of high-temperature oxide superconductors. Oxide layers, for example, are LaO in the La system, BaO in the Y system, BiO double layers in the Bi system, and NdO in the Nd system and do not contain copper (hereinafter referred to as "non-copper oxide layer"). The atomic arrangement of these non-copper oxide layers is NaCl type (a typical ion crystal structure) or similar to NaCl type. The atomic arrangement of high-temperature oxide superconductors can be deemed to be a laminated structure of non-copper oxide layers and CuO_2 faces (Figure 1). As hereinafter noted, CuO_2 faces are good electrical conductors and the atomic arrangement of high-temperature oxide superconductors can be deemed to be a laminated structure of ion crystals and metals.

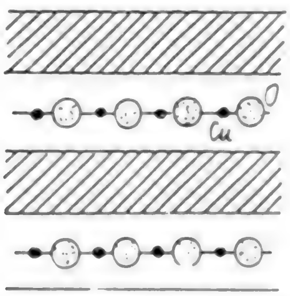

Figure 1. Laminated Structure of Non-Copper Oxide Layer (slanting line) and CuO_2 Faces (Section)

The laminated structure shown in Figure 1 greatly differs in physical properties between the horizontal and vertical directions. In the case of the Y system, for example, the ratio of vertical to horizontal directions in regard to electrical resistance amounts to 10^5 times. In the case of Bi system, Bi-O double layers are insulators [1].

The electrical conductivity and large anisotropy of CuO_2 faces are features peculiar to all high-temperature oxide superconductors.

(2) Electron Theory on CuO_2 Face

(i) Strong Correlations

Figure 2 shows a CuO_2 face. It appears that Cu and O have been ionized into Cu^{+2} and O^{-2}, respectively. However, the CuO_2 face causes negative charges to excessively increase. Such excessive electric charges, however, balance with positive charges on non-copper oxide layers sandwiching CuO_2 face, thus neutrality being maintained as a whole.

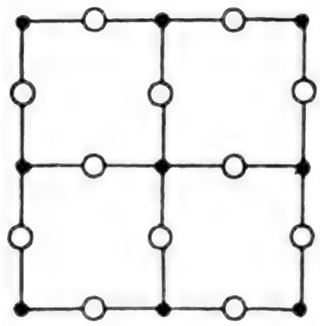

Figure 2. CuO_2 Face--Black circle: Cu^{+2}, white circle: O^{-2}

With respect to the electron arrangement of the ion nucleus, Cu^{+2} is $3d^9$, and O^{-2} is $2s^2p^6$ and, therefore, the total number of electrons per CuO_2 becomes an odd number. If two (upward and downward spins) electrons per level are packed from the lower energy level, one electron finally remains and shows the highest energy condition. According to the solid electron theory, the Brillouin zone is filled with two electrons per atom (or unit) and becomes an insulator unless bands overlap with each other. Where the number of electrons per atom (or unit) is one, the Brillouin zone becomes unconditionally metallic. CuO_2 faces, however, are insulators as can be known from the fact that $CaCuO_2$ crystals obtained by unlimitedly putting CuO_2 faces in layers are insulators [2]. Ca of $CaCuO_2$ is called an "oxygen deficient face" and is an atomic layer necessary to put CuO_2 faces in layers, as in the case of Ca in Bi and Tl systems and Y in the Y system, respectively.

Why are the CuO_2 faces of $CaCuO_2$ insulators? According to the most reliable theory, strong correlations between electrons cause CuO_2 faces to become insulators. Each electron senses each other's electric charge and is subject to strong Coulomb repulsion force. This is called "correlations." Therefore, if an electron existing at the Cu^{+2} position, as shown in

Figure 2, tries to move to the adjacent Cu^{2+} position, the electron is subject to a strong Coulomb repulsion force from the electron already present at the Cu^{2+} position and is forced back to the original Cu^{2+} position. The same occurs in both the horizontal and vertical directions. As a result, electrons lose their mobility. This is slightly similar to the fact that pure Si and Ge composing semiconductors are insulators. In the case of semiconductors, carriers are introduced by doping impure atoms that are different in atomic value, and thus electrical conductivity is obtained.

(ii) Doping of Carriers

With respect to high-temperature oxide superconductors, it is also necessary to dope carriers into CuO_2 faces. Holes are supplied to CuO_2 faces by Ba^{+2} (substituting La^{+3}) in the La system, O^{-2} (O on a CuO chain sandwiched by BaO layers instead of O on a CuO_2 face) in the Y system, maybe BiO in the Bi and TI systems, and O^{-2} excessively contained in TIO layers. In the Nd system, Ce^{+4} substituting Nd^{+3} acts as a carrier and supplies electrons. The supply of 0.1 to 0.3 carriers per Cu atom causes electrons to become mobile and the material to become a superconductor (metallic).[3] Lack of carriers causes the dependency of electric resistance on temperatures to become semiconducting.

The presence of another condition on mobilizing has recently been found.[4] In other words, carriers do not directly move from Cu^{+2} to Cu^{+2} but move via O^{-2} (Figure 2). With respect to the high-temperature oxide superconductor ion bonding ability, differences in the Madelung energy of carriers at Cu^{+2} and O^{-2} position are thought to play a vital role. Where either Cu^{+2} or O^{-2} location is greatly stabilized by the static potential energy given by the surrounding ions, electrons stay at such position.

(3) Superconducting Characteristics

(i) Short Coherent Length ξ

The upper critical magnetic field Hc_2 of high-temperature oxide superconductors is extraordinarily large compared with that of metals. Regarding the Y system, for example, the application of a magnetic field in the in-c face direction and c axial direction causes $Hc_2(0)$ (0 = a value extrapolated to the absolute zero degree) to reach 222 T and 61 T, respectively. The upper critical magnetic field Hc_2 is a magnetic field when the entire specimen is packed to the full with quantum magnetic flux lines. (Magnetic flux is quantized and magnetic flux ϕ_0 per quantum magnetic flux line is $hc/2e = 2.07 \times 10^{-7}$ gauss-cm^2.) and the entire specimen undergoes phase transition to the non-superconducting state. If ξ (Ginsberg and Landau coherence length) is introduced as a target for the size of a non-superconducting region that is accompanied by quantum magnetic flux lines, Hc_2 can be represented by the following equation, because Hc_2 is equal to magnetic flux per unit area.

$$Hc_2(T) = \phi_0 / 2\pi \xi^2(T) \qquad (1)$$

where T = temperature

Hc_2 being large corresponds to ξ being small. In the case of the Y system, $\xi(0)$ = 25 to 35 Å in the in-c face direction and $\xi(0)$ = 7 to 8 Å in the c axial direction. ξ changes according to orientations, which shows anisotropy.

The coherence length ξ can be interpreted as follows: Supposing that a non-superconducting region exists in a superconductor, the effect of the superconducting state extends over the non-superconducting region to the degree of distance ξ. In other words, the non-superconducting region having dimensions smaller than ξ is actually connected to the superconducting region, in a superconducting state. Short ξ shows that defects such as grain boundaries easily result in weak bonding regions. Consequently, while the grain boundaries of high-temperature oxide superconductors cause the critical current density Jc to lower, they can become barrier layers to Josephson junctions. Such fact has already been reported.

(ii) Flux Creep

Even in the case of Class 2 superconductors, a superconducting current flows through the superconducting portion. However, if an electric current is applied to a high-temperature oxide superconductor under a magnetic field, an electric resistance easily occurs. Supposing the area density of quantum magnetic flux lines is n, the magnetic flux density can be given by $B = n\phi_0$. The moving of these quantum magnetic flux lines at velocity v causes a voltage to be generated in the superconductor according to the following Faraday's electromagnetic induction law. This is merely caused by an electric resistance having occurred in the superconductor.

$$E = B \times v/c \qquad (2)$$

Figure 3 shows electric resistance/temperature curves.[23] A magnetic field is applied to the direction vertical to the c face in both the Y and Bi systems. If external magnetic flux B is increased at a fixed temperature, Lorentz force applied to quantum magnetic flux lines grows, v thereby becomes larger, and E also becomes larger, as equation (2) shows. The application of a magnetic field in both the Y and Bi systems, therefore, causes the electric resistance/temperature curves to shift to the low temperature side. As can be seen from Figure 3, quantum magnetic flux lines are pinned more strongly in the Y system than in the Bi system.

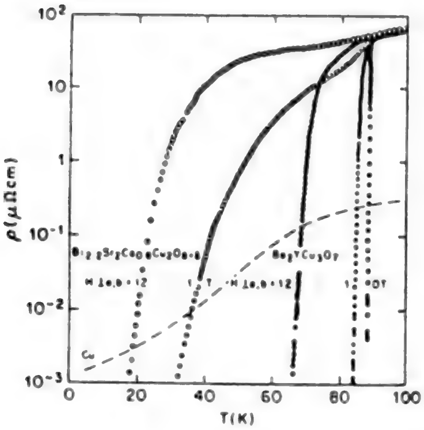

Figure 3. Electric Resistance ρ, Temperature T Curves.
Magnetic Field: c Axial Direction.
Black Marks: Y System, White Marks: Bi System
A magnetic field is shown in each $\rho \cdot T$ curve at units of T. Broken lines show copper $\rho \cdot T$ curves. The effect of the magnetic field is larger in the Bi system than in the Y system.[23]

It is thought that quantum magnetic flux lines are tightly pinned to control their movement. It is also thought that regions where the base phase superconducting characteristics are different from each other--such as non-superconducting precipitate phases--dislocations, grain boundaries, twin boundaries, and point defects act as pinning centers. However, in the case of high-temperature oxide superconductors, the true nature of pinning centers still remains unclear. To put high-temperature oxide superconductors to practical use, it is important to identify the true nature of pinning centers. Short coherence length ξ and large anisotropy, however, are complicating the problems.

(iii) Magnetic Flux Lattice and Pinning

Quantum magnetic flux lines regularly line up and lower their energy. If the section of such magnetic flux line lattice is sampled, it can be shown that quantum magnetic flux lines form a triangular lattice (Abrikosov lattice). Such regular arrangement arises from a repulsive force acting between quantum magnetic flux lines. If quantum magnetic flux line density n is given, the distance between quantum magnetic fluxes becomes the largest in the case of triangle lattice.

The potential energy barrier arising from the pinning center that acts on a quantum magnetic flux line is assumed to be u_p. It should be noted, however, that it is not sufficient to calculate only quantum magnetic flux line creep rate based on correlations between u_p and thermal energy kT because quantum

magnetic flux lines form triangle lattices and the hardness (elastic constant) of lattices has an effect on creep rate. Further, changes in the condition of quantum magnetic flux line distribution according to temperatures will greatly affect the creep rate. Figure 4 shows both two-dimensional and three-dimensional distributions of quantum magnetic flux lines.[5]

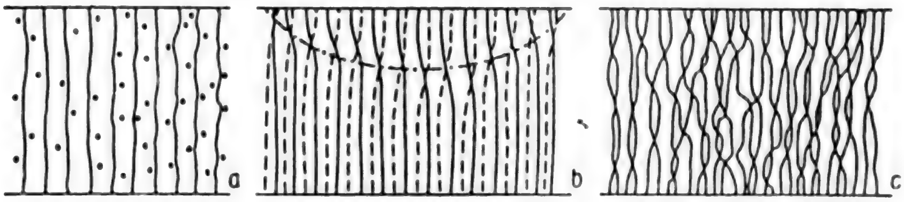

Figure 4. Section on Quantum Magnetic Flux Lines (solid lines, broken lines) and Pinning Actions (when a magnetic field was applied to the direction vertical to thin film face)
(a) Two-dimensional distribution. (The rigidity rate of quantum magnetic flux lines is large with respect to pinning force.) Black circles show pinning centers. (b) Where a spiral dislocation (alternate long and short dash lines) has occurred from the magnetic flux lattice surface. (c) Where many spiral dislocations have been introduced. Three-dimensional distribution.[5]

Figure 4 (c) shows a limit when dimensions Lc and Rc in the coherent region (Lc in the magnetic flux line direction, Rc in the vertical direction) in Figure 4 (a) have become gradually smaller. The pinning force f_p in such coherent region can act in both positive (f_p) and negative ($-f_p$) directions based on the relative position between quantum magnetic flux lines and pinning centers. In other words, the statistical sum (that is, fluctuation) of pinning force in the coherent region becomes a collective pinning force.[6] Such concept was applied by Kes to high-temperature oxide superconductors.[7] Literature [8] should be referred to concerning simple explanations in this connection.

(4) Mechanical Property

Specific features of the high-temperature oxide superconductor crystal structure were mentioned in 2 (1). The lattice constant is generally in a relation of $a \sim b \ll c$. Consequently, the Burgers vector size "b" of dislocation is small inside the c face and is extremely large in the c axial direction. The elastic energy of dislocation lines is proportional to μb^2 (μ = shear elasticity modulus). This makes it difficult to introduce dislocations having Burgers vector components, in the c axial direction. The number of independent slipbands, therefore, is limited to two slipbands

inside a c face. Within such limit, it is almost impossible to plastically deform multi-crystals. In the case of the Y system, the Burgers vector of slipband dislocations actually faces in a or b axial direction.[9]

As mentioned above, the bonding of high-temperature oxide superconductors is controlled by the CuO_2 face, and a large anisotropy is hidden in the crystal structure. The bonding of high-temperature oxide superconductors, therefore, is expected to be easily cleaved along non-copper oxide layers. Experience shows that the bonding of high-temperature oxide superconductors is liable to be cleaved in Y [10] and Bi systems. Slip deformation inside a c face, therefore, is placed in a competitive relation with breaking deformation arising from cleavage along the c face. In many cases, strong processing involves the cleavage breaking of crystal grains. It is necessary, therefore, to recover the bonding between the grain pieces of crystals broken by heat treatment, etc. after processing.

3. Problems with Practical Use

(1) c Face Orientation

A superconducting current easily flows along the in-c face direction due to the laminated structure of non-copper oxide layer/CuO faces. Further, the coherence length ξ in the direction along the c face is longer than in the vertical direction. For these reasons, the c face orientation of crystals can be thought to be an initial step to achieve a high critical current density Jc.[11] As effective processes for c face orientation, strong processing,[12] physical evaporation, chemical evaporation, etc. are currently widely known. Further, nucleus formation and growth directions are controlled in the process of solidifying materials from the melted liquid condition. This process proves to be effective. As examples of nucleus formation and growth, Bi based 2212 phase[13] on a silver tape and one-directional solidification in a Y system can be cited, respectively.[14] In this case, the direction of growth is in-c face direction (c axis is vertical to the solidification direction). Therefore, even if a crystal grain boundary is formed, c faces (of crystal grains) sandwiching the grain boundary come into contact with each other. This process properly uses the anisotropy of crystal growth. Thus, the development of a forming method fully utilizing the anisotropy originally provided for high-temperature oxide superconductors must be studied in the future. The layer-by-layer growth of thin films corresponds to the development of such forming method.[11]

(2) Control of Anisotropy

The quantum magnetic flux line lattice of a matter whose anisotropy is large is liable to be put in the state shown in Figure 4 (c). It moves to the state shown in Figure 4 (a), with a decrease in anisotropy (see [8]). A Bi system having a larger anisotropy and a Y system whose anisotropy is weaker than that of the Bi system tend to approach the two-dimensional arrangement shown in Figure 4 (c) and (a), respectively. Figure 4 (a) (2-dimensional

state) shows that the pinning forces tend to be statistically positive and negative and to negate each other. Figure 4 (c) (3-dimensional state) shows that each pinning center effectively pins quantum magnetic flux lines. If attention is paid to this point, the pinning potential Up per coherent region becomes as follows.

$$Up(Bi) < Up(Y) \tag{3}$$

The pinning force Fp per unit volume becomes as follows.

$$Fp(Bi) > Fp(Y) \tag{4}$$

Small Up of a Bi system causes large flux creep. To increase Up, it is necessary to relax the anisotropy of the Bi system and, thereby, control the anisotropy to the same level as that of Y system. The control of anisotropy is a major subject to be studied in the future. The relaxation of anisotropy appears to affect the mechanical properties and to facilitate slips in the c axial direction.

(3) Pinning Center

High-temperature oxide superconductors should be used at temperatures exceeding the liquid nitrogen temperature. With regard to even Y systems being fully studied compared with other systems, the real nature of pinning centers remains uncleared. Some experiments show that the real nature of pinning centers may be twin boundaries. Some experiments, however, show that no twin boundaries work.[15] Experiments using samples prepared by the quench and melt growth (QMG) process developed by Murakami, et al., deduce that pinning centers may be distortions and dislocations occurring in a microscopic 211 phase (about 0.29 μm) or in the area around such 211 phase.[16] Meanwhile, $YBa_2Cu_3O_{7-\delta}$ films prepared by the chemical vapor deposition (CVD) process show a high Jc (77.3 K, 6.5 X 10^4 A/cm^2 at 27T).[17] Microscopic inclusions (CuO riched phase) existing between layers, however, are estimated to be pinning centers, and the size of such inclusion is about 0.05 μm.[18]

These results show that no pinning centers common to $YBa_2Cu_3O_{7-\delta}$ exist. If the size of an inclusion is less than about 0.1 μm, there is the large possibility that any non-superconducting phase is an effective pinning center. This appears to be a future research subject.

(4) Preparation of Thin Film

Efforts are being made to process superconducting materials into thin films mainly in Y and Bi systems. Preparation of thin films by the sputtering or vacuum evaporation process involves problems with low oxygen partial pressures inside the vacuum chamber and substrate temperatures. A critical oxygen partial pressure exists per substrate temperature. At temperatures below such critical temperature, $YBa_2Cu_3O_x$, $Bi_2Sr_2CaCu_2O_x$, or CuO is

decomposed.[19,20] The critical oxygen partial pressure is nearly equal in regard to the above three substances (Figure 5). The decomposition or otherwise of CuO faces contained common in the above three substances affects the stability of these substances. This agrees with the size of a and b axes of a high-temperature oxide superconductor being controlled by Cu-O bonding (see 2(1)(i)). The initial thin film preparation conditions (oxygen partial pressure and substrate temperature) are in the upper right half region shown in Figure 5.

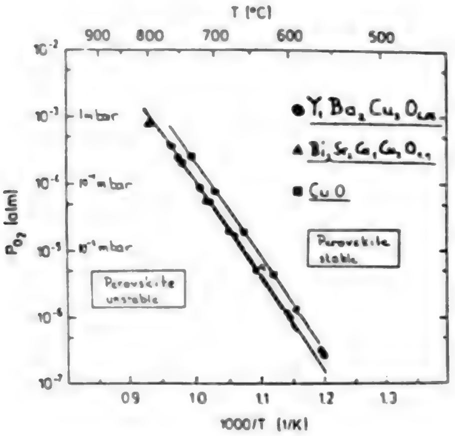

Figure 5. Critical Oxygen Partial Pressure Causing Decomposition Reactions Regarding $YBa_2Cu_3O_{6.05}$, $Bi_2Sr_2Ca_1Cu_2O_{7-9}$, and CuO[19,20]

The next step in preparing thin films is to introduce carriers. In the case of a Y system, the Bando group's reactive vacuum evaporation process can be cited as an example of success.[22] Here, the preparation of Bi based 2223 phase thin films that still involves many problems is mentioned. Table 1 presents examples where researchers have to date comparatively succeeded in processing superconducting materials into thin films,[11] though such examples are limited to only the case where the low temperature process was used. The table shows that the Tc zero is low, that is, 0 to 70 K in the state of evaporation, irrespective of the type of manufacturing processes. Annealing of the materials after evaporation causes the Tc zero to be greatly improved, but the Tc zero never reaches 110 K. Experiments on such as the presence or otherwise of a modulation structure and chemical shift [24] of inner-core electron level of Bi, Sr, Ca, and Cu show that oxygen is insufficient in the state of evaporation and that a mixture of Sr and Ca remains after annealing, and Tc is thereby lowered. It appears that the lack of oxygen causes oxygen atoms on CuO_2 faces to be eliminated and O vacancies to be formed.[11] It is a future research subject, therefore, to remove O vacancies and to prevent the conversion of Sr and Ca into alloys, where superconducting materials are processed into thin films.

Table 1. Bi Based 2223 Thin Film: Fabrication Method, Heat Treatment, and Superconducting State Transition Temperature

Fabrication Method		As deposited		Post-annealed		Ref.
		Tsub(°C)	Tc zero(K)	Temp.(°C)×Time(hr)	Tc zero(K)	
rf or dc magnetron sputtering	cosputt.	700	35	885 × 1 *	95	a
	Bi/SrCu/CaCu/SrCu	650	~10	850 × 5	~80	b
	Bi/Sr-Ca-Cu-O	665	10-30	810 × 1	82	c
ion beam sputtering	Bi-O/Sr-Ca-Cu-O	605	45	— –	—	d
thermal evaporation	coev.	630	~70	400 × 1	78	e
laser ablation	Bi-O/SrCuOy /CaCuOy/SrCuOy	480	0 *	820 × 5 *	~80 *	f

—— :not specified * : private communication

a) H.Itozaki et. al. : 2nd Workshop on High Temp. Superconducting Electron Devices (1989) Hokkaido .p293
b) H.Adachi et.al. : Jpn. J. Appl. Phys. 27 (1988) L1883
c) K.Nakamura et.al. : Jpn. J. Appl. Phys. (submitted)
d) J.Fujita et.al. : Appl. Phys. Lett. 54 (1989) 2364
e) T.Sato et.al. : Appl. Phys. Lett. 55 (1989) 702
f) M.Kanai et.al. : Appl. Phys. Lett. 54 (1989) 1802

Where a 2223 phase is prepared by the stacking process at a substrate temperature of 600°C, the 2223 phase is completely decomposed to a 2212 phase by annealing at 760°C for one hour. At a substrate temperature of 665°C, however, the 2223 phase is maintained at a stable state after annealing at 760°C for one hour.[21] It is also important to study whether the use of the thin film preparation processes at lower temperatures is compatible with thermal stability.

4. Conclusion

The microscopic characteristics of high-temperature oxide superconductors were described in this paper from the material science, and the following topics were discussed.

(1) Structural features

(2) CuO face electron theory

(3) Superconductivity characteristics

(4) Mechanical property

These, however, have posed various research subjects that cannot be found in conventional metal superconductors. The subjects herein discussed are:

(1) Plane c orientation

(2) Control of anisotropy

(3) Pinning center

(4) Processing of superconducting materials into thin films

A breakthrough is expected to be able to be made in these research subjects.

5. References

1. Tanaka, M., et al., Nature 339 691 (1989).

2. Creaves, C., Nature 334 193 (1988).

3. Torrance, J. B., et al., Rhys. Rev. Lett. 61 1127 (1988).

4. Torrance, J. B. and Metzger R., Rhys. Rev. Lett. 63 1515 (1989).

5. Brandt, E. H. and Essmann, U., phys. stat. sol. (b) 144 13 (1987).

6. Larkin, A. I. and Ovchinnikov, Yu. N., J. Low Tem. Phys. 34 409 (1979).

7. Kes, P. H. and van den Berg, J., in "Flux Pinning and Thermally Activated Depinning in Single Crystals of High Temperature Superconductors," edited by A. V. Narlikar (Nova Science Pub., Commack, N Y).

8. Keiichi Ogawa, meeting report: 9th Symposium "Behavior of High Temperature Superconductor Critical Current and Magnetic Flux Line," NSMF NEWS 1989-12-1 issue p 13 (Unexplored Scientific Technology Association).

9. Ikeda, S., et al., Jpn. J. Appl. Phys. 26 L729 (1987).

10. Hatano, T., et al., Jpn. J. Appl. Phys. 26 Ls74 (1987).

11. Ogawa, K., et al., in "Fabrication and Characterization of BSCCO Films," Proceedings of the 2nd International Symposium on Superconductivity (1989) (to be published).

12. Okada, M., Jpn. J. Appl. Phys. 27 L1715 (1988).

13. Kase, J., et al., Appl. Phys. Lett. (submitted).

14. Togano, K., pers. note.

15. Masaki Suenaga, quoted Literature 8.

16. Masato Murakami, Journal of Japan Ceramics Association (manuscript requested).

17. Watanabe, K., Appl. Phys. Lett., 54 575 (1989).

18. Ymane, H., et al., in "High Tc Superconducting Oxide Films Prepared by CVD," Proceedings of the 2nd International Symposium on Superconductivity (1989) (to be published).

19. Bormann, R. and Nolting, J., Appl. Phys. Lett. 54 2148 (1989).

20. Bormann, R. and Nolting, J., in Critical Oxygen Pressure for the "in situ" Preparation of High Tc Superconducting Thin Films," International Conference on Materials and Mechanisms of Superconductivity (1989).

21. Nakamura, K., et al., Jpn. J. Phys. 1990 (in press).

22. Terashima, T., et al., Jpn. J. Appl. Phys. 27 L91 (1989).

23. Palstra, T. T. M., et al., Appl. Phys. Lett. 54 763 (1989).

24. Kohiki, S., et al., Phys. Rev B39 4695 (1989).

Critical Current and Behavior of Magnetic Flux

906C7513B Tokyo KO ON CHODENDOTAI NO JITSUYOKA E NO TENBO in Japanese
17 Jan 90 pp 11-14

[Article by Teruo Matsushita, Engineering Dept., Kyushu University]

[Text] 1. Preface

Critical current characteristics hold the key to the practical use of high-temperature superconductors. Further, the use of superconductors at the nitrogen temperature involves large thermal energy and, therefore, magnetic flux creep is expected to have serious effects on the achievement of practical use. Magnetic creep is a phenomenon in which quantized magnetic flux caught by pinning centers is thermally activated, crosses the pinning energy barrier, and thereby moves.[1] Thus, even a small amount of current causes magnetic flux flow to occur and thereby critical current to become zero.[2] Also, even if a limited critical current is measured, permanent current lowers such limited critical current and attenuates with the passage of time.[3] These phenomena have already been reported. The possibility or otherwise of practical application of high-temperature superconductors, therefore, depends on how much the effect of such magnetic flux creep can be reduced. To this end, it is necessary to increase pinning energy. Is it possible, however, to increase such pinning energy in the case of high-temperature superconductors, in view of principles? To what extent must pinning energy be increased? These points are discussed in this paper.

2. Depth of Magnetic Flux Creep and Pinning Potential

It is assumed that quantized magnetic flux or its flux bundle is caught by the pinning potential as shown in Figure 1. In this case, the "irreversibility line" on a magnetic field temperature plane, where the critical current density Jc determined based on an appropriate electric field standard E = Ec (for example, 100 μV/m) becomes zero, can be given[2] by the following equation, according to the magnetic flux creep theory.[1]

$$U_0 = k_b T \ln(B a \nu_0 / E_c) \qquad (1)$$

where K = Boltzmann constant
a = distance between pinning potentials
ν_0 = flux bundle oscillation frequency

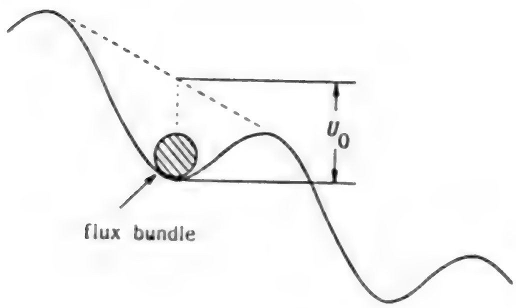

Figure 1. Flux Bundle Caught by Pinning Potential
The potential slope arises from Lorentz force operating.

The critical current density is zero on the higher temperature and higher magnetic field side compared with the curve determined by Equation (1). According to Yeshurun and Malozemoff,[2)] the magnetic field where Jc becomes zero at 77 K is merely 0.7 T in a Y-Ba-Cu-O single crystal.

It is also assumed that an ideal critical current density is Jc where there are no thermal disturbances and that such critical current density has been achieved at $t = t_0$. The later attenuation of the permanent current density with the passage of time can be represented by the following equation.[3)]

$$J = J_{c0}\,[1-(k_BT/V_0)\ln(t/t_0)] \tag{2}$$

Equation (2) shows that the larger the pinning potential depth U_0, the smaller the attenuation of the permanent current density. Also, the irreversibility line moves to the higher temperature and higher magnetic field side as U_0 grows. It can be said, therefore, that U_0 is an important parameter, indicating the size of effects of magnetic flux creep, and that the process for increasing U_0 is an important subject to be studied.

3. Depth of Pinning Potential

It is known that the pinning potential in regard to quantized magnetic flux lattice per unit volume is generally written as $(1/2)\,\alpha_L u^2$ with respect to the displacement u of magnetic flux, using Labusch parameters[4)] α_L. Therefore, if the size of a pinning potential is assumed to be di and the flux bundle volume to be V, the following equation can be given.

$$U_0 = (1/2)\,\alpha_L d_i^{\,2} V \tag{3}$$

A correlation of $\alpha_L di = Jc_0 B$ exists between the above quantities and Jc_0. It is thought that the flux bundle volume is determined based on the elastic correlative distance of magnetic flux lattice. If the elastic correlative distance of magnetic flux in the vertical and horizontal directions are

assumed to be ℓ_{44} and ℓ_{66}, respectively, these can be given by $\ell_{44} = (C_{44}/\alpha_L)^{1/2}$ and $\ell_{66} = (C_{66}/\alpha_L)^{1/2}$ using elastic constants C_{44} and C_{66} based on magnetic flux lattice bending and shear. In the case of strong pinning that interests us, however, ℓ_{66} becomes smaller than the magnetic flux lattice distance $a_f = (2\phi_0/\sqrt{3}B)^{1/2}$ (ϕ_0 = magnetic flux quantum) and a_f substantially gives a flux bundle size in the horizontal direction. Consequently, the following equation can be obtained.

$$V \simeq \ell_{44} a_f^2 \tag{4}$$

Pinning centers herein pose problems in high-temperature superconductors. The real nature of pinning centers resulting in the current Jc remains unclear. This makes it difficult to estimate the type of pinning centers to be introduced in the future. Jc values, therefore, are estimated herein using empirical experiment facts. In other words, a semi-theoretical approach is carried out herein. The use of the microscopic alternate current magnetic field superimposing process has made it possible to know, in regard to many superconducting specimens, that d_i is proportional to magnetic flux lattice distance a_f. ζ is herein used as adjusting parameters for materials (theoretically[6] $\zeta > 4$) and d_i is represented by the following equation.

$$d_i = a_f/\zeta \tag{5}$$

By substituting Equations (4) and (5) and $C_{44} = B^2/\mu_0$ for Equation (3), the following equation can be obtained.

$$U_0 = (8\phi_0^{\,7} J_{c0}^{\,2}/27\sqrt{3}\zeta^6 \mu_0 B)^{1/4} \tag{6}$$

In other words, under the category of strong pinning, U_0 is proportional to the 1/2 power of Jc_0.

4. Irreversibility Line

To obtain irreversibility lines using Equations (1) and (6), it is necessary to know U_0, that is, dependency of Jc_0 on magnetic field and temperature. Jc_0 is a critical current density in cases where there are no thermal disturbances and is expected to be able to be introduced by thermal dynamic discussions as in the case of metal based low-temperature superconducting materials. From this, it is estimated that scale rules, as in the case of metal based superconducting materials, can be established in regard to the dependency of Jc_0 on magnetic field and temperature. The following equation, therefore, is used herein.

$$J_{c0}(B, T) = AB_{c2}^{\,m-\gamma}(T)\,[1 - B/B_{c2}(T)]^{\delta} \tag{7}$$

where A = constant
m, γ, δ = parameters

Equation (7) is then substituted for Equation (6) and is approximated as being $Bc_2(T) = Bc_2(0)(1-T/Tc)$. Equation (1) becomes as follows.

$$\frac{K}{T}\left(1-\frac{T}{T_c}\right)^{(m-\gamma)/2}\left[1-\frac{BT_c}{B^*_{c2}(0)(T_c-T)}\right]^{\delta/2} = B^{(3-2\gamma)/4} \tag{8}$$

K is a constant and can be obtained using the following equation.

$$K = 0.835\,\frac{[AB^{*\,m-\gamma}_{c2}(0)]^{1/2}}{\zeta^{3/2}\ln(B\nu_0 a/E_c)} \tag{9}$$

The logarithm in Equation (9) is about 20 and is a quantity that does not greatly change. Supposing that two-dimensional pinning centers like twinning planes operate in a Y system, it can be estimated that $\gamma = 1/2$ and $m = 2$ based on the example[7] of pinning arising from the crystal interface in Nb_3Sn. Using this, it is assumed that the irreversibility field Bi at T = 77 K is fully smaller than Bc_2. Then, the following dependency is obtained.[8] Such dependency is the same as that of the results of experiments conducted by Yeshurun and Malazemaff.[2]

$$B_i = \left(\frac{K}{T_c}\right)^2\left(1-\frac{T}{T_c}\right)^{3/2} \tag{10}$$

To what extent can Bi be enlarged by strengthening pinning? We are interested in such point. The strength of a pinning center (elementary pinning force) is generally proportional to $Bc^2\xi/2\mu_0$ as Bc being a thermal dynamic magnetic field and ξ being a coherence length. Such value is about 0.3[9] at 77 K for a Y system, on the assumption that Nb_3Sn at 4.2 K is 1. This shows that pinning is not so potentially weak. Incidentally, Nb-Ti at 4.2 K is about 0.06. It is thought, therefore, that a critical current density of about 2×10^{10} A/m^2 at 77 K and 5T can be fully achieved from the thermodynamic standpoint.[10] Thus, ζ is estimated to be about 6[8] for specimens having strong pinnings. From this, where a magnetic field exists in a-b face, it can be estimated that Bi $\simeq$74T. The ratio of such Bi $\simeq$74T to real Bc_2 remains unknown, but such value is fully large from the standpoint of practical use. In other words, such value can easily clear the conditions allowing limited Jc values to exist up to a fully high magnetic field. Actually, a large Jc can be maintained up to 27T in regard to Y based CVD films, and Bi is estimated to be about 62T.[11]

5. Attenuation of Permanent Current

The attenuation of permanent current can be given by Equation (2). $\zeta = 6$ is assumed for a Jc_0 of 2×10^{10} A/m^2 at 77 K and 5T, as already noted. Under this temperature and magnetic field, $U_0 = 7.44 \times 10^{-20}$ J (0.47 eV). This shows that permanent current attenuates about 11.8 percent in one hour. Further, use of materials under a higher magnetic field or use of materials having a lower Jc_0 shows a more conspicuous attenuation of permanent current. From this, it can be thought that magnetic flux creep has a large effect on

the attenuation of permanent current. The attenuation of all currents, however, can be avoided by setting the operating current at a level considerably lower than the critical current value. From this sense, the achievement of a Jc_0 value to a certain extent appears to make it possible to apply high temperature superconductors, for example, to energy handling equipment, etc. Even where a permanent current attenuates 25 percent per hour, such permanent current value can be maintained for 3600^2 seconds $\simeq 5$ months by reducing the working current to 50 percent. In this case, however, the current distribution in superconducting wires changes, as shown in Figure 2, with the passage of time, thus posing problems in cases where a certain accuracy is required for the magnetic field, as in the case of MRI and accelerators. It appears necessary, therefore, to take appropriate measures such as the reduction of a superconducting element wire diameter as much as possible.

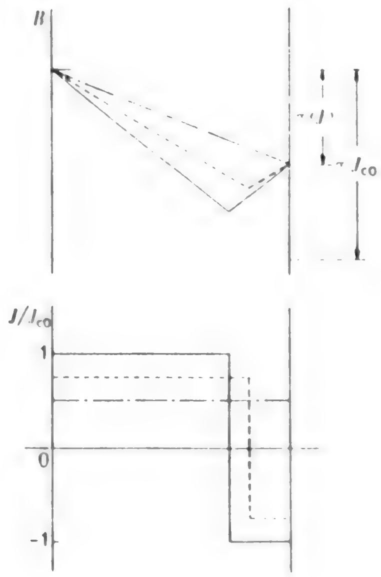

Figure 2. Changes in Magnetic Flux Distribution in Superconducting Wire (upper) and Current Distribution (lower)
Solid lines: at the time of current setting
Broken lines: at the time of 25 percent attenuation
Chain lines: at the time of 50 percent attenuation

The spread of resistance transition width in a magnetic field[12)] poses problems, although this matter is not directly related to practical application. The material temperature is gradually raised from the low temperature region and resistance occurs. Such resistance is thought to first occur when the critical current density rapidly lowers due to magnetic flux creep and becomes equivalent to the conveyance current density. In

other words, magnetic flux motion occurs and resistance thereby occurs. Such magnetic flux motion gives a difference between the resistance generating temperature and critical temperature, that is, the resistance transition width. From this, it is thought that the major mechanism determining resistance transition curves is a magnetic flux flow as in the case of metal based superconducting materials. According to such concept, if critical current density Jc and flow specific resistance ρ_f are given, the electric field at any current density J can be obtained by $E = \rho_f(J-Jc)$ and specific resistance $\rho = E/J$ can thereby be obtained. The low resistance region arising from a pure magnetic flux creep is not discussed in this paper. The use of the Bardeen-Stephen model for ρ_f [13] makes it possible to obtain resistance transition curves shown in Figure 3. From using this simple magnetic flux flow model, an anisotropy of resistance transition curves can be obtained, based on Bc_2 anisotropy, and swellings appear on the way of curves. These agree qualitatively with the results of experiments and it can be understood that resistance transition mainly arises from magnetic flux flows. Precisely speaking, it is observed that the flow specific resistance deviates from the Bardeen-Stephen model and the causes for such deviation remain unknown.

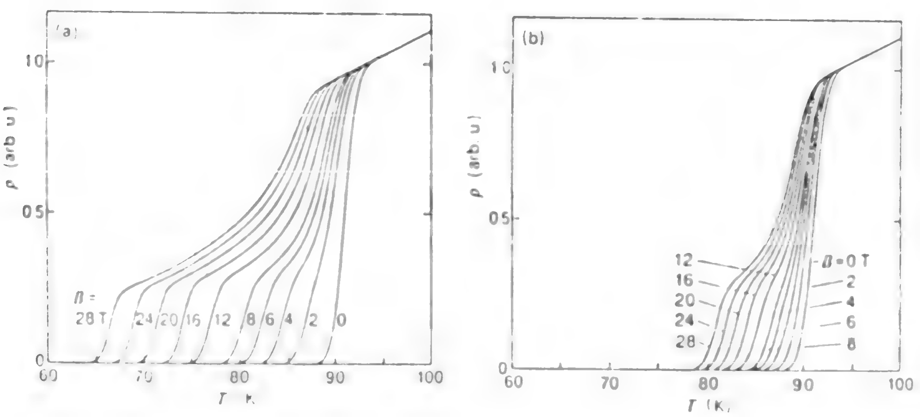

Figure 3. Example of Resistance Transition in High-Temperature Superconductor
(a) Shows a case where the magnetic field is in parallel with c axis.
(b) Shows a case where the magnetic field is vertical to c axis.

Literature

1. P. W. Anderson: Phys. Rev. Lett. 9 (1962) 309.

2. Y. Yahurun and A. P. Malazemoff: Phys Rev. Lett. 60 (1988) 2202.

3. A. M. Campbell and J. E. Evetts: Adv. Phys. 21 (1972) 299.

4. R. Labusch: Crystal Lattice Defects 1 (1969) 1.

5. K. Yamafuji, et al.: Physica C 159 (1989) 743.

6. T. Matsushita: Jpn. J. Appl. Phys. 20 (1981) 1955.

7. E. J. Kramer: J. Appl. Phys. 44 (1973) 1360).

8. T. Matsushita: to be published in Physica B.

9. T. Matsushita: to be published in Proc. 2nd Int. Symp. on Superconductivity, Tsukuba, 1989.

10. T. Matsushita: Jpn. J. Appl. Phys. 27 (1988) L1712.

11. K. Watanabe, et al.: Jpn. J. Appl. Phys. 28 (1989) L1417.

12. Y. Iye, et al.: Jpn. J. Appl. Phys. 26 (1987) L1057.

13. J. Bardeen and M. J. Stephen: Phys. Rev. 140 (1965) A1137.

Superconducting Thin Film Technology

906C7513C Tokyo KO ON CHODENDOTAI NO JITSUYOKA E NO TENBO in Japanese
17 Jan 90 pp 15-18

[Article by Hideo Itozaki, Itami Research Laboratory, Sumitomo Electric Industry Co., Ltd.]

[Text] 1. Preface

Since the discovery of high-temperature oxide superconductors, materials having a higher critical temperature are being sought and studies are being conducted concerning already discovered superconductors. Meanwhile, studies are being positively carried out to apply superconductors having a critical temperature higher than that of liquid nitrogen to energy and electronic fields. In the energy field, research to process high-temperature superconductors into wires is actively proceeding. The critical current density is amounting to several ten thousand A/cm^2. Meanwhile, for applications to electronics, the processing of high-temperature superconductors to thin films and upgrading their quality are also being positively studied. At present, it is possible to prepare thin films having a critical current density of several million A/cm^2. In this paper, the author describes the achievement of high Jc using the sputtering process (so far used by the author) for high-temperature superconducting thin films and the future outlook for the superconducting thin film manufacturing technology.

2. Current Status of Superconducting Thin Film

It is indispensable for the electronic field to process materials used for electronic equipment to thin films. A variety of thin film manufacturing processes (developed with the progress of the semiconductor manufacturing technology) have to date been used to study the processing of high-temperature superconductors into thin films. As processes often used, the sputtering process (physical evaporation process) and the vacuum evaporation process can be cited. These processes have recently been improved and, therefore, the use of such improved processes is being currently studied, together with the laser evaporation process. Further, chemical evaporation processes such as thermal CVD and OM-CVD are being developed. The sputtering process is used to process Y,[1-3], Bi,[4] and Tl[5] based superconductors, each

having a Tc of liquid nitrogen or higher, into thin films having a high critical current density. In this paper, therefore, the author studies the characteristics of superconducting thin films so far obtained and describes the current status of superconducting thin film development.

Table 1 presents the major superconducting characteristics--critical temperature (Tc) and critical current density (Jc (77.3 K)) at a zero magnetic field liquid nitrogen temperature of 77.3 K--of YBCO, BSCCO, and TBCCO high-temperature superconducting thin films so far obtained.

Table 1. Characteristics of YBCO, BSCCO, and TBCCO Thin Films

	YBaCuO	BiSrCaCuO	TlBaCaCuO
Tc	90 K	105 K	115 K
Jc (77.3 K)	4 M A/cm^2	3.4 M A/cm^2	3.2 M A/cm^2

Tc almost equivalent to the values so far reported in regard to sintered materials has already been obtained. Also, an extremely large critical current density, exceeding 3,000,000 A/cm^2, has been achieved, compared with a Jc of several ten thousand A/cm^2 reported on bulk materials and wires. Described below are the electrical characteristics, thin film structures, etc. of YBCO thin films, the study of which is being positively carried out. Using the RF magnetron sputtering process, thin films were formed on an MgO single crystal (100) substrate at a substrate temperature of about 650°C and were annealed for about one hour using oxygen of 900°C or higher.

(1) Electrical Characteristics of YBCO Superconducting Thin Film

Figure 1 shows the temperature characteristics of resistivity of thin films formed by the sputtering process. Such characteristics greatly change according to the crystallizing ability and oxygen content of thin films. Satisfactory thin films showing high Jc indicate a considerably low electric resistance and a linear temperature dependency that tends to proceed to the origin of the coordinate axes (Figure 1). Figure 2 shows the dependency of Jc on the magnetic field. Jc lowers with an increase in the strength of an applied magnetic field, though it tends to slowly lower compared with bulk materials. A Jc of about 1 million A/cm^2 is maintained at 1 tesla.

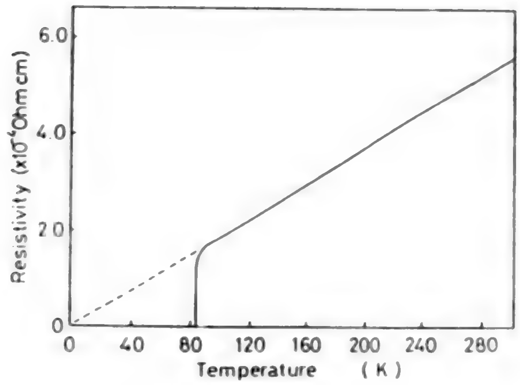

Figure 1. Dependency of YBCO Superconducting Thin Film Electric Resistance on Temperature

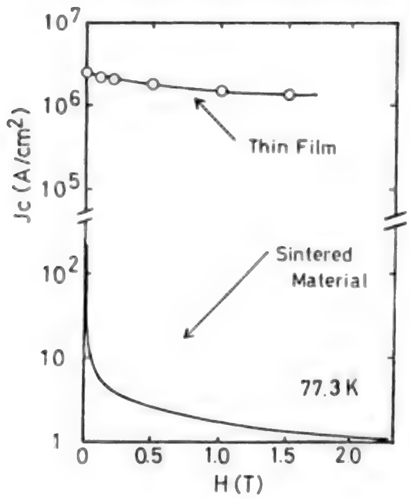

Figure 2. Dependency of YBCO Superconducting Thin Film Jc on Applied Magnetic Field Strength

(2) Structure of YBCO Superconducting Thin Film

Figure 3 shows a high resolution YBCO superconducting thin film SEM surface photograph. An extremely smooth surface has been formed on an epitaxially grown thin film. The surface irregularity falls within a range of less than several tens of A. X-ray diffraction shows a sharp peak (00n). Along with this, a streak pattern appeared in RHEED, and this shows that the thin film has a single crystallizing ability. High Jc thin films have a single crystallizing ability. Thin films, in which crystal grain boundaries

are almost not observed, were obtained. It appears that the lack of crystal grain boundaries (regulating a superconducting current) has resulted in a high Jc.

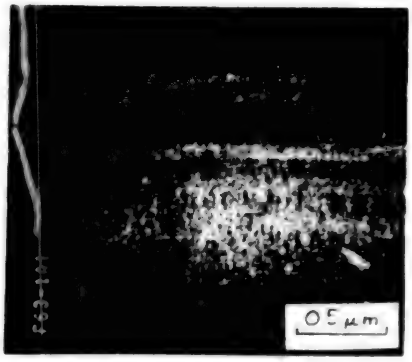

Figure 3. Highly Resolved YBCO Superconducting Thin Film SEM Surface Photograph

A microscopic structure of single crystal superconducting thin film was observed using a transmission electron microscope (Figure 4).[6] The electron diffraction figure shows a spot pattern and the range of observation appears to have a crystal orientation structure.

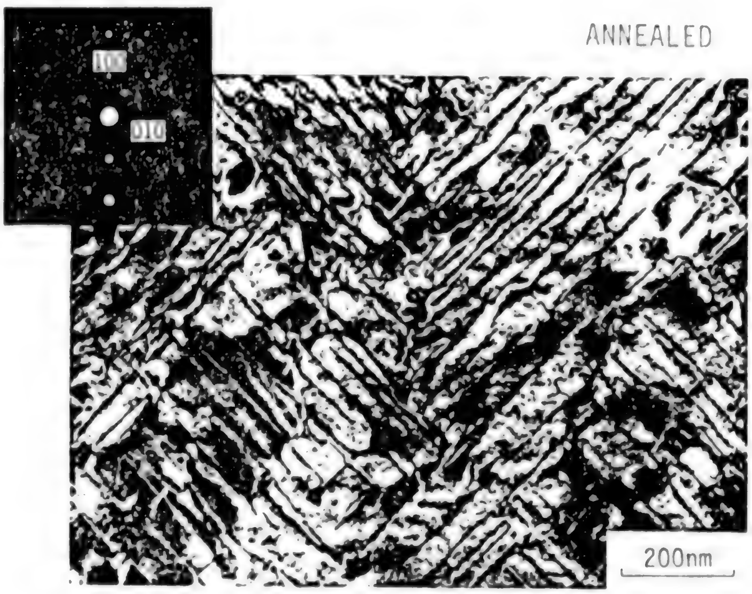

Figure 4. YBCO Superconducting Thin Film Photographed Using Transmission Electron Microscope

In Figure 4, however, many defects can be seen in regard to a bright-field of vision of a transmission electron microscope. Linear defects are oriented in the [110] direction. In addition, a high-resolution observation of defects shows a continuous atomic alignment. Such linear defects, therefore, can be thought to be twin boundaries. Such twin crystals are thought to arise from a slight difference in the length between the a and b axes of a superconductor. Further, many irregular contrasts can be seen in the figure and each crystal face slightly inclines. These show that residual distortions are introduced on a large scale. In addition, many dislocations and microscopic linear defects can be observed. As shown in Figure 2, superconducting thin films also maintain a high current density in a high magnetic field. It is necessary, therefore, to pin magnetic flux lines entering superconducting thin films. It appears that these highly dense introduced defects serve as magnetic flux line pinning centers.

(3) As-grown Superconducting Thin Film and High-Speed Film Formation

So far, the Tc of high-temperature superconducting thin films has been low immediately after formation. Formed films, therefore, were annealed for a fixed time by introducing oxygen into the chamber after formation. Further, formed films were annealed in a high-temperature (about 900°C) oxygen atmosphere to raise the Tc to 80 K or higher. Such heat treatment, however, causes reactions between the superconducting thin film and substrate and should preferably be avoided. It has recently become possible to obtain high Tc and high Jc superconducting thin films without using the above heat oxidation treatments. This appears to have resulted from the development of a technology in which thin films are placed in a fully oxidized state during growing by feeding activated oxygen to the thin film surfaces.

Further, a technology for forming thin films at higher speed is being developed, together with the said as-grown technology. It is reported that thin films having a Jc of more than 1,000,000 A/cm^2 were obtained using as-grown thin films. Data on such reports are shown in Figure 5 in terms of a function of Jc and film forming speed. The film forming speed has been improved from several A/s to more than ten l/s. This is making it possible to obtain high Jc thin films by higher-speed film formation. The author has been able to obtain as-grown thin films (epitaxially grown by feeding oxygen--converted into rf plasma--to thin films under growing) by a high-speed film formation of 6 A/s, using the evaporation process.

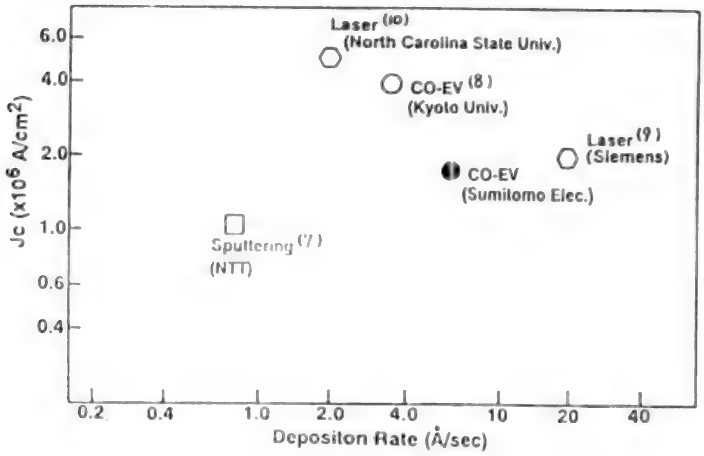

Figure 5. Jc and Film Formation Speed of As-Grown YBCO Superconducting Thin Film

As mentioned above, the technology for processing high-temperature superconductors into thin films has so far been developed. At present, extremely smooth, epitaxially grown single crystal thin films are being obtained at comparatively high speed using as-grown thin films without high-temperature annealing treatment.

3. Future Outlook for Superconducting Thin Film

The positive research and development of high-temperature superconducting thin films has made it possible to obtain epitaxially grown thin films. It appears, therefore, that studies on practical use of superconducting thin films will more positively proceed in the future.

In the electronic field, studies on processing superconducting thin films for devices are about to be carried out positively. The technology for processing superconductors into thin films is expected to be connected with the semiconductor manufacturing processes. To this end, it is necessary to develop technologies such as lower temperature process, growing of superconducting thin films on semiconductor substrates, hetero-epitaxial growth, and laminating. In view of processing superconducting thin films for devices, it is thought that bonding technology will be studied and that microscopic processing technology will also proceed.

Studies are also being carried out concerning the use of high-temperature superconducting thin films as superconducting wires, where it is necessary to form thin films on lengthy substrates. In this case, polycrystals are presumed to be used as substrate materials. At the present moment, high Jc thin films can be obtained solely on single crystal substrates. It appears

that the development of a technology allowing high Jc thin films to be obtained will also be carried out in regard to polycrystalline substrates.

References

1. Y. Enomoto, T. Murakami, M. Suzuki, and K. Moriwaki, Jpn. J. Appl. Phys. 26, L1248 (1987).

2. T. Terashima, K. Iijima, K. Yamamoto, Y. Bando, and H. Mazaki, Jpn. J. Appl. Phys. 27, L91 (1988).

3. S. Tanaka and H. Itozaki, Jpn. J. Appl. Phys. 27, L622 (1988).

4. H. Itozaki, K. Higaki, K. Harada, S. Tanaka, N. Fujimori, and S. Yazu, ed. by K. Kitazawa and T. Ishiguro, Advances in Superconductivity, Nagoya, 1988 (Apringer-Verlog, Tokyo, 1989) p 599.

5. S. Yazu, ed.by K. Kitazawa and T. Ishiguro, Advanced in Superconductivity, Nagoya, 1988 (Apringer-Verlog, Tokyo, 1988) p 563.

6. H. Itozaki, Proceeding of the 2nd Int. Symp. on superconductivity (ISS'89), Nov. 1989, Tsukuba, Japan.

7. H. Asano, M. Asahi and O. Michikami, Jpn. J. Appl. Phy. 28, L981 (1989).

8. T. Terashima, K. Iijima, K. Yamamoto, J. Takada, K. Hirata, H. Mazaki, and Y. Bando, J. Crystal Growth, 95, 617 (1989).

9. B. Roas, L. Schultz, and G. Endres, Appl. Phys. Lett. 53, 1557 (1988).

10. R. K. Singh, J. Narayan, A. K. Singh, and J. Krishnaswamy, Appl. Phys. Lett. 54, 2271 (1989).

Application of High-Temperature Superconductor to Electronics

906C7513D Tokyo KO ON CHODENDOTAI NO JITSUYOKA E NO TENBO in Japanese
17 Jan 90 pp 19-22

[Article by Takeshi Kobayashi, Engineering Dept., Osaka University]

[Text] 1. Preface

High-temperature oxide superconductors are very attractive substances because their critical temperature is extremely high compared with conventional metal-based superconductors. They are characterized as follows:

- Liquid nitrogen can be used as a cooling medium.
- Ultra high frequency waves based on highly condensed energy are used.
- Properties peculiar to the materials concerned are effectively utilized.

Satisfactorily utilizing these features, high-temperature superconductors are expected to be widely applied to electronic equipment. The crystal structure, however, is complicated and it is desired that rapid progress be made in the crystal manufacturing technology for the practical use of high-temperature superconductors.

Crystals of a series of high-temperature superconductors (Tc > 77 K) such as YBaCuO are not only plural system compounds, but also are far from cubic systems. In addition, an anisotropy resistant to electrical and optical properties can be observed. From the engineering standpoint, it appears slightly difficult to manufacture and use high-temperature superconductors. It is a great pleasure, however, for men to have been able to obtain such characteristic electronic materials. Struggles with the new materials that involve many difficulties in research are not only our greatest pleasure but also our obligation. Immediately after the discovery of such high-temperature superconductors, the author advocated the usefulness of the "hetero-epitaxial technology," while expecting that research is widely carried out on such technology. The number of research institutes involved with the hetero-epitaxial growth appears to have recently increased, and this gives me a great pleasure. High-temperature oxide superconductors are multielement crystals and should be handled in the same manner as for the compound semiconductor system. It is the hetero-epitaxial technology that

properly utilizes compound semiconductors. It is well known that a marked progress in the hetero-growth technology has caused the hetero-epitaxial technology to receive much attention and to be applied to a wide variety of fields. Similarly, establishment of the hetero-epitaxial growth technology promises us that the specific features of high-temperature oxide superconductors are utilized for application to electronics. Meanwhile, new probes can be offered to physical property research. From both the engineering and physical science standpoints, the hetero-epitaxial technology is expected to play a vital role.

The hetero-epitaxial laminated structure is a key technology indispensable to achieving the practical use of Josephson junctions that represent superconducting devices. In addition, the hetero-epitaxial laminated structure may play a key role in creating new superconducting devices, in which the new functions of oxide superconductors are utilized. As examples, the electric field effect of the YBaCuO-MIS structure, recently discovered by our group, can be cited. This research is also completely supported by the hetero-epitaxial technology.

This paper describes advantages and disadvantages in the application of high-temperature superconductors to electronics. Then, examples of attractive applications and specific matters in question are made clear. Points so far attained and problems to be resolved in the future are also described.

2. Specific Features of High-Temperature Oxide Superconductors

- Multielement compound crystal:

    - Abundant replacement of elements (superconducting, non-superconducting, insulating, magnetic, non-magnetic, etc.).
    - Difficult to adjust stoichiometry.
    - Under high-quality crystal performance, high-temperature superconductivity can be obtained. (Achievement of highly advanced film forming technology and process technology.)

- Anisotropy:

    - Local semi two-dimensional electric conductivity (application to functional device).

- Low carrier concentration:

    - Highly efficient modulation of superconductivity due to modulation of carrier density (injection, electric field effect, light irradiation).
    - Improvement of transparency.
    - Weak superconductive bonding of grain boundaries (grain boundary Josephson).
    - Increases in high frequency surface resistance.

- Short coherence length:

  - Achievement of superconducting thin films.
  - Weak superconductive bonding of grain boundaries.
  - Indispensable completeness of surface and interface crystals.

The progress of application of high-temperature superconductors to the electronic field is slow, contrary to our expectation, because the above mentioned problems in material engineering are preventing smooth applications. In addition, establishment of the epitaxial growth technology for compound crystals having a complicated structure is taking much time. The conventional Nb based superconducting devices were typical thin film devices. Generally, thin film devices are those formed by films accumulated in a single layer or in laminated layers using the evaporation and sputtering processes. The characteristics of the above high-temperature superconductors, however, do not allow high-temperature superconductors to be used as thin film devices. The effective use of high-temperature superconductors cannot be considered without high-quality epitaxial or hetero-epitaxial growth. YBCO easily separates oxygen by high-temperature processing or ion irradiation. It has been made clear that the effect of ions accelerated to 500 eV makes it possible to completely separate Cu-O one-dimensional chain O atoms.

3. Requirements for Applying High-Temperature Superconductor to Electronics

3.1 Josephson Junction

Hopes are being placed on the achievement of superconductor-insulator-superconductor (SIS) Josephson junctions. In other words, crystals are arranged in such a way that the conduction surface is located vertically with respect to the insulator (I) layer and that planes on both sides accurately face each other. Further, a superior superconductivity must be maintained in the vicinity of the interface between I layers and superconducting layers. Double hetero-epitaxy, although it is being currently developed, can comply with this requirement.

Instead, grain boundary Josephson junctions (GBJJ) and SNS devices, in which the I layer is replaced by a non-superconductor N, are being positively studied. GBJJs are devices that can be currently operated at the highest temperature. They, however, use polycrystalline films, and noise arising from magnetic flux quantum creep at grain boundaries and abnormal increases in high-frequency surface resistance are posing problems. IBM, however, manufactured a Tℓ based GBJJ-SQUID for experiments and has confirmed operations superior to an Nb-SQUID (rf) operating at 4.2 K. This is a topic of great interest to us.

3.2 High-Frequency Line, Wiring

Superconductors show a complete zero resistance with respect to dc current but show resistance with respect to a high-frequency current. An ac magnetic field enters from superconductor surfaces, induces an ac electric field, accelerates semi-particles in the superconductor, and a loss thereby occurs. This is surface resistance. Such surface resistance increases as the square of a frequency. It is expected, however, that at 77 K, such surface resistance becomes a value smaller than the Cu line maintained at the same temperature up to a hundred and several ten GHz. Results as estimated were obtained by using epitaxial films and single crystals. Polycrystalline films, however, showed results worse than Cu lines because grain boundaries and large defects in crystals cause an abnormal resistance. It is required, therefore, that an epitaxial technology capable of being used for semiconductor circuit wiring and inter-chip wiring be urgently established.

In AT&T's Bell Labs, it has been observed that 40 ps dual pulses can be transmitted through a 5-cm YBCO strip line almost without involving distortions. In the case of Cu lines, a large attenuation of signals and a large deterioration of waveforms could not be avoided. In this case, epitaxial films also proved to be highly effective.

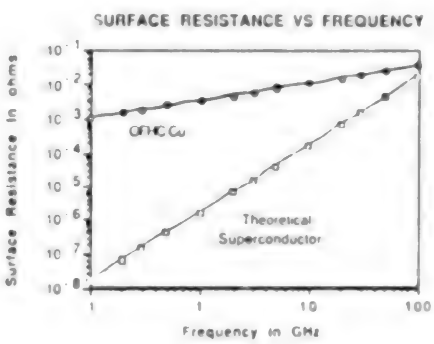

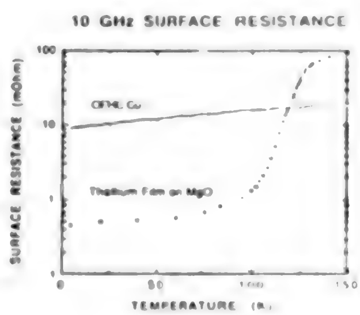

3.3 Magnetic Shielding and Acceleration Cavity

One of the main uses of the superconducting Meissner effect is for magnetic shielding, although this results in geometrically large shapes. Superconductors prepared using polycrystals have many grain boundaries, and external magnetic fields are trapped in such grain boundaries. Further, the creeping of trapped magnetic flux quanta gives noise to the measuring system.

Microwave acceleration cavities are indispensable for particle acceleration. Efforts are being made to reduce cavity loss as much as possible in order to use microwave acceleration cavities with a large electric power. For such purpose, superconducting cavities are used. In this case, however, the aforesaid surface resistance poses problems.

In any event, the above equipment is large in shape and it is necessary to develop a new technology to manufacture single crystal films (having a large area) that can be supplied to such large equipment.

3.4 High-Temperature Superconducting Three-Terminal Device (transistor)

Development of three-terminal devices having superconducting characteristics is our long-cherished dream. (Several devices have to date been proposed and manufactured for experiments but have not yet been put into practical use.) There is a movement to manufacture superconducting field-effect transistors (that are familiarized in semiconductors) by using the low carrier density of high-temperature oxide superconductors. Preliminary experiments have already been started.

It is necessary to prepare epitaxial films whose electric conduction surfaces are properly arranged to improve the characteristics and to establish a technology for manufacturing a laminated structure, in which the level of the interface between gate insulating films and high-temperature superconductors is reduced as much as possible. The use of the hetero-epitaxial technology is indispensable for such purpose.

4. Current Status of Hetero-Epitaxial Technology

As mentioned above, the hetero-epitaxial growth technology plays a vital role in applying high-temperature superconductors to electronic equipment. The hetero-epitaxial growth technology, however, remains unmatured and this gives us a feeling that the use of high-temperature oxide superconductors involves difficulties. Semiconductor lasers may not have been put into practical use without the hetero-technology.

So far, the author's group has pursued the possibility of YBCO-MgO-YBCO double hetero-epitaxial growth. As a result, it has become possible to prepare hetero-structures consisting of a variety of crystal orientation combinations as shown below.

A super lattice, in which YBCO/LSCO was laminated lattice by lattice at two cycles (48 Å), has recently been manufactured. Further, super thin films, in which YBCO was grown at a thickness of about 20 Å, have been manufactured and critical temperatures ranging from 50 to 60 K have been achieved. In other words, research has made progress to the extent that high-temperature superconductors consisting of, so to speak, only surfaces can be satisfactorily operated.

For application to electronic equipment, it is necessary to utilize the real characteristics of high-temperature superconductors. Such application will be started in the near future. To this end, it is desired that research be conducted in a fully scientific manner.

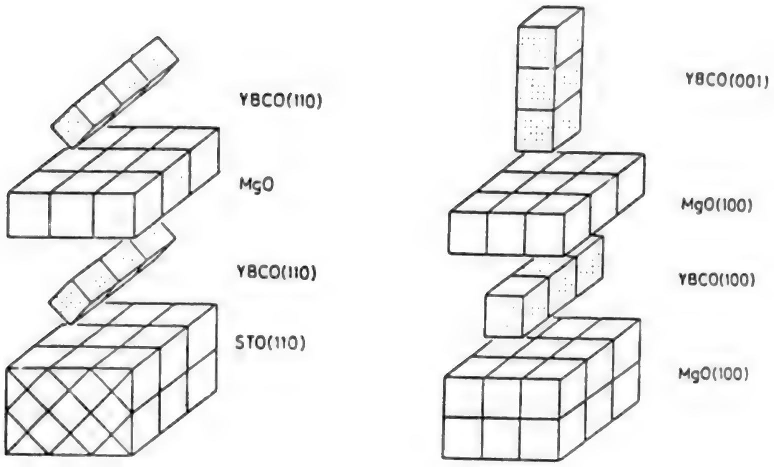
YBCO(110)
MgO
YBCO(110)
STO(110)
YBCO(001)
MgO(100)
YBCO(100)
MgO(100)

Processing of Superconductors into Superconducting Wires

906C7513E Tokyo KO ON CHODENDOTAI NO JITSUYOKA E NO TENBO in Japanese
17 Jan 90 pp 23-26

[Article by Tsukasa Kono, Key Material Research Laboratory, Fujikura, Ltd.]

[Text] 1. Preface

Most technologies for applying superconductors to energy technology are based on coils. Research on the conventional metal group superconducting materials, therefore, has been carried out with emphasis on the technology for processing superconducting materials into superconducting wires (hereinafter referred to as "wire manufacturing"), which were applied to coils. High-temperature superconductors are still in the process of initial research and have not yet reached the stage in which wire manufacturing technology can be fully discussed, as in the case of the metal group superconducting materials. Since the discovery of La based superconductors, however, various researches have been conducted concerning the wire manufacturing technology in which the characteristics of high-temperature superconductors are utilized. The superconducting characteristics of wires are gradually being improved, although such characteristics are not superior to those obtained by the thin film preparing technology used for manufacturing devices.

In this paper, an outline of the wire manufacturing technology and the details of research being challenged by each research institute are introduced to review the current and future research and development state.

2. Outline of Wire Manufacturing Process

The superconducting wire manufacturing process can be classified into three types, based on the properties of ceramics: solid phase process (emphasis laid on powder sintering); liquid phase process (emphasis laid on powder melting); and vapor phase process (emphasis laid on thin film formation). On the basis of the characteristics of these processes, therefore, studies have to date been carried out concerning the wire manufacturing process. Figure 1 shows an example of classification of the above processes.

- Solid Phase Process
  - Direct Work
    - Hot Press
    - Hot Isostatic Press
  - Powder Method
    - Metal Sheathed Drawing
    - Binder Addition
      - Doctor Brade
      - Extrusion
      - Screened Printing
  - Solid State Reaction
    - Internal Oxidation
    - Surface Diffusion
    - Solid State Diffusion
- Liquid Phase Process
  - Liquid Quenching
    - Liquid Oxide Quenching
    - Liquid Oxide Drawing
  - Solution Method
    - Sol-Gel
    - Suspension Spinning
  - PLasma Spraying
- Vapor Phase Process
  - Physical Vapor Deposition
    - Sputtering
    - Laser Ablation
    - Vacuum Deposition
    - Ion Cluster Beam
  - Chemical Vapor Deposition

Figure 1. Classification of Wire Manufacturing Process

At the initial stage of research, researchers showed a marked tendency to use various processes at random for wire manufacturing. However, as knowledge on the anisotropy and crystal orientation of high-temperature superconductors was gradually obtained, research on processes has been carried out based on a story. The various views of the story, however, may be arranged as per Figure 2.

3. Current Status of and Challenge to Wire Manufacturing

The current status of wire manufacturing using the sheath process of the solid phase process, the melting process of the liquid phase process, and the thin film process of the vapor phase process is described below, from among the wire manufacturing processes shown in Figure 1.

(1) Sheath Process

Many studies are being carried out for the sheath process of the solid phase process. This process is characterized not only by the advantages on the processing side, but also by the advantages as wires as described below.

- Advantages on processing side:
  - The conventional metal processing technology can be used.
  - The simplest equipment can be used.

- Advantages as wires:
  - The sheath process is suitable for manufacturing lengthy wires.
  - A comparatively large amount of electrified current can be taken.

Crystal	- Removal of impurities (removal of foreign matter and foreign phase) - Control of oxygen content (transformation of YBCO system phase) - Control of grain boundaries (weak bonding and magnetic flux flow, reduction of grain boundaries $\longrightarrow$ single crystallization)

Bulk materials	- Density of sintered material (securing of current path) - Crystal orientation (anisotropy: ab axes $\Leftrightarrow$ c axis) - Homogeneity (short ξ : wide heterogeneity of substance $\longrightarrow$ heterogeneous superconductivity) - Introduction of pins (microscopically scattered phase, others)

Wires	- Processing for orientation (rolling: conformity of ab axes with processing direction) - Processing for grain boundary control (reduction of diameter partial melting, directional solidification) - Lengthy homogeneity (securing of homogeneous superconductivity) - Processing of orientated thin films to tape conductors (matching with base material, high orientation)

Figure 2. Wire Manufacturing Process Research Story (Themes to be conquered and their details, and actual examples)

The dependency of a critical current on a magnetic field, however, is large; the degree of crystal orientation cannot be raised as in the case of thin films. Rises in critical current density are often retarded due to the inclusion of a large amount of grain boundaries. Critical current density (Jc) of the wires obtained by this process is still lower by about two digit numbers compared with that of thin films. Utilizing the specific features of wires whose critical current (Ic) is high, 20 tape wires were processed to

cables. As a result, it has become possible to obtain a critical current of 150 A.[1] Table 1 presents the maximum critical current density (so far reported) of wires.

Table 1. Critical Current Density (OT, 77 K) of Wires Manufactured by Silver Sheath Process

Component	Research Institute	Dimensions (unit: mm)	Jc (A/cm^2)
Y-Ba-Cu-O	Sumitomo Electric Industries, Ltd.	0.5tx3.6Wx30L	$4.1x10^3$
Bi-Pb-Sr-Ca-Cu-O	Furukawa Electric Co., Ltd.		$3.5x10^4$
Tl-Pb-Ca-Ba-Cu-O	Sumitomo Electric Industries, Ltd.	0.15tx3.0Wx40L	$1.08x10^4$

In the case of the YBCO system, the critical current density has not yet been improved compared with 4.1×10^3 A/cm^2 (OT, 77 k)[2] reported in 1988 as the sheath process. However, there is an example in which the critical current density showed 1×10^3 A/cm^2 (1T, 77 K)[3] as a result of the directional solidification technique having been applied after processing. This can be said to be an attempt to conquer the lowering of Jc arising from grain boundaries, using the melting process.

Meanwhile, the BSCCO system accounts for the largest portion of the top data recently obtained by the sheath process. As the highest value, 3.5×10^4 A/cm^2 (OT, 77 K)[4] has been reported. YBCO and TBCCO systems are bulk crystal structures, whereas the BSCCO system is a flake-shaped crystal structure. Crystals, therefore, are liable to be lined up in the rolling direction due to the rolling force applied during the reduction of diameters. Thus, it appears that an electric current has come to easily flow due to a high orientation. This is the reason that the Jc of BSCCO system is high. In the case of wires of 3.5×10^4 A/cm^2, Jc values were arranged based on the degree of the crystal orientation, and a high Jc is reported to have been obtained by achieving an orientation of 99 percent.

(2) Melting Process

The melting process served to easily orient crystals in YBCO materials first obtained by the melt textured growth (MTG) process.[5] In addition, high Jc

values, 1.7 x 10^4 A/cm^2 (OT, 77 K) and 4.0 x 10^3 A/cm^2 (1T, 77 K), were reported under a magnetic field and received much attention. Later, with regard to YBCO system, non-superconducting phase (211 phase) microscopic particles were scattered in a YBCO superconductor using the quench and melt growth (QMG)[6] process, and pinning centers were introduced. Thus, it was revealed that such pinning centers may serve to improve Jc.

Jc = 1 x 10^4 A/cm^2 (1T, 77 K) was an important value in view of securing Jc under a magnetic field, although this value was introduced from the magnetization characteristics. No attempts for wire manufacturing using the above process have yet been reported, and many hopes are placed on such attempts. Trials, however, are currently being carried out for bulk disk magnets. To improve the magnetic field characteristics of a disk magnet, the melting powdering melting growth (MPMG)[7] process has been developed. This process adopts concepts on the powder process as an improved process; it introduces midway powdering mixing, and pressing processes to more effectively carry out 211 phase dispersion. Magnetic fields of 1T and 0.16T at 4.2 K and 77 K, respectively, are reported to have been generated on an experimental basis.

Superconducting materials placed in a melted state are shaped into wires and are processed into a solidified state without changing the shape, thus superconducting wires are obtained. This process can be easily conceived as a general melting process. For the YBCO system, however, the phases are liable to be separated in a melted state, thus involving difficulties in obtaining a large stable volume of superconducting phases. Various researches, therefore, are being conducted on the melting process in the BSCO system, in which superconducting phases can be stably obtained compared with other systems. Research is also being conducted on the process in which solidified phases are formed on metal tape to prepare tape conductors, processes in which fibers are prepared by the drawing process or the spinning process, etc.

To process BSCCO superconductors into fibers, studies are being carried out on the laser pedestal process,[8] μ-cz process,[9] etc. BSCCO fibers of 2.5 mm dia. x 90 mm long and 0.32 mm dia. x 150 mm long have already been obtained using the respective processes. Both processes show similar characteristics as described below.

- Laser pedestal process: Tc = 87 K, Jc = 3.07 x 10^3 A/cm^2 (OT, 77 K)
- μ-cz process: Tc = 84 K, Jc = 3.17 x 10^3 A/cm^2 (OT, 77 K)

Fibers prepared by the μ-cz process are reported to have been satisfactorily oriented in the longitudinal direction. Wire manufacturing using fibers, however, poses many problems, such as procedures for manufacturing lengthy wires and study of compounding to improve the critical current value.

The above two processes aim at improving Jc by forming BSCCO system low Tc phases (2212 phase). It is difficult to change a high Tc phase (2223 phase)

to a single phase, in the BSCCO system. It is more difficult to achieve a high Jc of a high Tc phase. Consequently, a low Tc phase that can be stably obtained is formed and the crystal orientation is improved as much as possible to achieve a high Jc. These are being intensively carried out.

(3) Thin Film Process

It is necessary for specific features such as highly oriented films, high Jc films, and single crystal films on single crystal substrates, to be able to be reproduced on metal tape without involving any changes. This holds the key to success in wire manufacturing using the thin film process. It can be said that research on wire manufacturing using the thin film process (being currently studied) is proceeding under the above story. There are many thin film processes other than those shown in Figure 1, and they are used mainly in the semiconductor field. Wire manufacturing is thought to be being studied using the thin film process suitable for each research institute, although the final target of each institute is to form thin film semiconductors on a lengthy metal tape. Most research, however, is currently concentrated on how satisfactory superconductors can be formed on a single crystal substrate, as basic research on processes. An attempt is also being made to form superconducting thin films on metal tape, although it is short tape.

Table 2 presents the processes that have already been reported as wire manufacturing research.

Every material given in Table 2 is a short specimen, still in the process of basic research, and appears to become future large themes. One of the purposes of wire manufacturing using the thin film process is to secure a bar about 1 m in length that has the following characteristics. This makes it possible to obtain wires having a critical current of several 10 A, and thereby to carry out basic study on electricity application technology.

- Dimensions of a superconductor: 10 μt x 5 mmW
- Jc of a superconductor: 2×10^4 A/cm^2 (0 to about 1T, 77 K)
- Ic of a superconductor: several 10 A

(4) Prospects for Wire Manufacturing

The current status of research on wire manufacturing using the solid phase, liquid phase, and vapor phase processes was reported in this paper. Although the processes used by the individual researchers may differ from each other, the final target is to develop wires having characteristics that can be applied to electricity technology. One such final target can be arranged as per Table 3.

Table 2. Wire Manufacturing Using Thin Film Process

Thin Film Process	Base material/ buffer/superconductor	Tc(K)	Jc(OT, 77 K)	Literature
Sputtering process (RF magnetron)	Hastelloy/YSZ/YBCO Hastelloy/MgO/YBCO	83 80.4	220 A/cm2 200	10 11
Chemical evaporation process	Hastelloy (0.1t)/-YBCO (5μt)	82	80	12
Ion cluster bean process (ICB)	Silver polycrystal/-/YBCO (0.4 μt)			13
Laser evaporation process (ArF excimer)	Hastelloy/SrTiO3/YBCO (0.2t) (0.5 μt) (1.5 μt)	81	500	14

Table 3. Target of Wire Manufacturing (example)

		First Step	Second Step	Third Step
Target Value	Wire	$Jc=2x10^4 \sim 10^5 A/cm^2$ (1T, 77 K) $Ic=10 \sim 50A$ (1T, 77 K) Line length: 1 m	$Jc=10^5 A/cm^2$ (5T, 77 K) $Ic-50 \sim 100A$ (5T, 77 K) Line length: 10 m	$Jc=10^5 A/cm^2$ (10T, 77 K) Ic=100A (10T, 77K) Line length: 100 m or longer
	Coil	Bm=1T Ln2 operation	Bm=5T LN2 operation	Bm=10T LN2 operation
Common subjects		Reproducibility, homogeneity, distortion resistance characteristics, bonding technology		

Some materials are already in the first step, but can be said to be considerably before the first step, if their Jc, Ic, and bar length under a magnetic field are considered. At the second and third steps, only the cooling medium is changed from liquid helium to liquid nitrogen. Achievement of these steps, however, will require considerable time and a large breakthrough in problems such as clarification of the basic pin structure and magnetic flux movement structure, and a balance between anisotropy/orientation control and magnetic field direction, as high-temperature superconductors. Such breakthrough depends on the progress in the future research and development. Research is also being conducted on the possibility or otherwise of using high-temperature superconductor Hc2 for high magnetic field applications; such research is receiving much attention as a new type of research.

References

1. K. Sato, T. Hikata, H. Mukai, and H. Hitotsuynanagi, 2nd Int. Symp. on Superconductivity Nov (1989) WB-8.

2. M. Nagata, K. Ohmatsu, H. Hukai, T. Hikata, Y. Hosoda, N. Shibuta, K. Sato, H. Hitotsuynagi, and M. Kawashima, Proc. 1st Int. Symp. on Superconductivity, Aug (1989) 377.

3. M. Okada, R. Nishiwaki, T. Matsumoto, T. Kano, K. Aihara, and S. Matsuda, 2nd Int. Symp. on Superconductivity, Nov (1989) PWB-2.

4. N. Enomoto, H. Kikuchi, N. Uno, T. Hara, K. Okaniwa, and T. Yamamoto, 2nd Int. Symp. on Superconductivity, Nov (1989) PLN-14.

5. S. Jin, T. H. Tiefel, R. C. Sherwood, M. E. Davis, R. B. van Dover, G. W. Kammlott, R. A. Fastnacht, and H. D. Keith, Appl. Phys. Lett. 52 (1988) 2074.

6. M. Murakami, M. Morita, K. Miyamoto, and S. Matsuda, Proc. Osaka Univ. Int. Symp. Oct (1988).

7. H. Fujimoto, M. Murakami, S. Gotoh, N. Koshizaki, T. Oyama, and Y. Shiohara, 2nd Int. Symp. on Superconductivity, Nov (1989) PWB-18.

8. K. Hayashi, H. Nonoyama, N. Nagata, and H. Hitotsuynagi, 2nd Int. Symp. on Superconductivity, Nov (1989) PWB-32.

9. A. Kurosaka, M. Aoyagi, H. Tominaga, O. Fukuda, and H. Osanai, Appl. Phys. Lett. 55 (1989) 390.

10. N. Harada, Sato, Yamamoto, Matsui, Nakajima, Narumi, Mashita, Ozaki, The Furukawa Electric's Review 84 (1989) 81.

11. Fukutomi, Akutsu, Tanaka, Asano, Maeda, 36th Appl. Phys. Society Lecture meeting, prelim. draft (1989) 4a-E-9.

12. Aoki, Yamaguchi, Kagawa, Kohno, 50th Appl. Phys. Society Lecture Meeting, prelim. draft (1989) 30 p-M-3.

13. Yamazaki, Yoshino, Tan, Yamashita, Ando, 50th Appl. Phys. Society Lecture meeting, prelim. draft (1989) 28p-PB-46.

14. K. Onabe, N. Sadakata, and O. Kohono, 2nd Int. Symp. on Superconductivity, Nov (1989) PLN-9.

- END -

END OF FICHE

DATE FILMED

21 Dec. 1990